Institute for Experimental Medical Research,
Oslo University Hospital and University of Oslo, Oslo, Norway.

KG Jebsen Cardiac Research Centre and
Center for Heart Failure Research, University of Oslo, Oslo, Norway

Chemokines in cardiac remodelling and heart failure, and their role in regulation of small leucine-rich proteoglycans in the extracellular matrix

Anne Wæhre

Dissertation for the degree of Philosophiae Doctor (PhD),
University of Oslo,
Oslo, Norway
2012

Series of dissertations submitted to the
Faculty of Medicine, University of Oslo
No. 1330

ISBN 978-82-8264-367-2

Cover: Inger Sandved Anfinsen.
Printed in Norway: AIT Oslo AS.

Produced in co-operation with Unipub.
The thesis is produced by Unipub merely in connection with the
thesis defence. Kindly direct all inquiries regarding the thesis to the copyright
holder or the unit which grants the doctorate.

Table of contents

Acknowledgement

The work for this thesis was carried out at the Institute for Experimental Medical Research at Oslo University Hospital Ullevål. First I would like to thank my supervisor Geir Christensen for excellent guiding and encouraging through this work. I am grateful for his continuous scientific support and for structured and critical, but friendly feedback.

I have had the pleasure of working with skillful colleagues, and would like to thank my co-authors Kristin B. Andersson, Dina Behmen, Johannes Bjørnstad, Kristin V.T. Engebretsen, Cathrine Husberg, William Louch, Ida G. Lunde, Ståle Nygård, Henriette Marstein, Biljana Skrbic, Ivar Sjaastad, Theis Tønnessen and Maria Vistnes at the Institute for valuable contributions. The collaboration with Pål Aukrust, Christen P. Dahl, Alexandra Finsen, Lars Gullestad, Bente Halvorsen, Leif E. Vinge and Arne Yndestad at the Research Institute of Internal Medicine at Oslo University Hospital Rikshospitalet has been very important. I am especially grateful for the prompt, constructive and enthusiastic feedback from Pål Aukrust. Furthermore, the contributions from Mohammad Shakil Ahmed, Håvard Attramadal, Henrik Brun, Denise Hilfiker-Kleiner, Martin Lipp, Christian Neukamm, Henrik Reims, Borghild Roald and Erik Thaulow are highly appreciated.

I am most grateful to Bjørg Austbø, Sigurd Boye, Ulla H. Enger, Hilde Dishington, Eli Wallem Gulliksen, Almira Hasic, Hilde Jarstadmarken, Heidi Kvaløy, Marianne Lunde, Per Andreas Norserg, Ole Kristoffer Olstad, Ellen Lund Sagen, Kalpana Sinnadurai, Vidar Skulberg and Roy Trondsen for highly appreciated biochemical and technical support. I would also like to thank Morten Eriksen, Carsten Lund, Siv Leng Tran, Siv Rong Tran, Ann-Kristin Josefsen and Marita Mathisen for expert animal care. Furthermore, I would like to acknowledge Ole M. Sejersted, Lisbeth H.Winer, Morten Eriksen, Ulla H. Enger and Jo-Ann F. Larsen for providing a working facility in good working order. I would also like to thank Øystein H. Horgmo at the Medical Photography Section at the Institute of Clinical Medicine, University of Oslo for making the figures in the thesis. I would also especially like to thank each and everyone at the Institute for making this an excellent place to work and for taking such good care of me.

Further, I appreciate the interest my family, my dear brother and parents, and my friends have shown in my work. I would especially like to thank my friend Teresia for sharing the ups and downs inherent in everyday research work.

Above all, I am deeply grateful to my wife Bente, my own Professor and my dearest and best friend. Finally, my beloved children, Nora Johanne and Halvor, you are everything to me. In short time we are all joined with “the little baby boy” who has been so kind through the final of this thesis.

Financial support was provided by the Norwegian Research Council, the Anders Jahres Fund for Promotion of Science, Rakel and Otto Kr.Bruun`s Fund, the Family Blix Foundation and Stiftelsen Kristian Gerhars Jebsen, Norway.

List of papers

The thesis is based on the following papers, which are referred to by their Roman numerals:

I. Vistnes M, Waehre A, Nygård S, Sjaastad I, Andersson KB, Husberg C, Christensen G. Circulating cytokine levels in mice with heart failure are etiology dependent. J Appl Physiol. 2010 May;108(5):1357-64.

II. Waehre A, Halvorsen B*, Yndestad A*, Husberg C, Sjaastad I, Nygård S, Dahl CP, Ahmed MS, Finsen AV, Reims H, Louch WE, Hilfiker-Kleiner D, Vinge LE, Roald B, Attramadal H, Lipp M, Gullestad L, Aukrust P, Christensen G. Lack of chemokine signaling through CXCR5 causes increased mortality, ventricular dilatation and deranged matrix during cardiac pressure overload. PLoS One. 2011 Apr 18;6(4):e18668.

III. Waehre A, Vistnes M, Sjaastad I, Nygård S, Husberg C, Lunde IG, Aukrust P, Yndestad A, Vinge LE, Behmen D, Neukamm C, Brun H, Thaulow E, Christensen G. Chemokines regulate small leucine-rich proteoglycans in the extracellular matrix of the pressure-overloaded right ventricle. J Appl Physiol. 2012 February 16; [Epub ahead of print].

IV.Engebretsen KVT*, Waehre A*, Bjørnstad J, Skrbic B, Sjaastad I, Behmen D, Marstein H, Yndestad A, Aukrust P, Christensen G, Tønnessen T. Decorin, lumican and their GAG-chain synthesizing enzymes are regulated in myocardial remodeling and reverse remodeling. *Submitted.*

Selected abbreviations

AB	Aortic banding
ANP	Atrial natriuretic peptide
BNP	Brain natriuretic peptide
CHPF	Chondroitin polymerising factor
CS	Chondroitin sulfate
CHSY	Chondroitin sulfate synthase
CSGALNACT	Chondroitin sulfate N-acetylgalatosaminyltransferase
DB	Debanding
DS	Dermatan sulfate
ECM	Extracellular matrix
ELISA	Enzyme linked immunosorbent assay
GAG	Glycosaminoglycan
GAPDH	Glyceraldehyde-3-phosphate-dehydrogenase
GUCH	Grown-up congenital heart disease
HF	Heart failure
KS	Keratan sulfate
LV	Left ventricle
MHC	Myosin heavy chain
MI	Myocardial infarction
MMP	Matrix metalloproteinase
PB	Pulmonary banding
RT-qPCR	Real-time quantitative polymerase chain reaction
RV	Right ventricle
SERCA2KO4w	Sarco(endo)plasmatic reticulum Ca^{2+}-ATPase, isoform 2 knockout, 4 weeks following gene deletion
SERCA2KO7w	Sarco(endo)plasmatic reticulum Ca^{2+}-ATPase, isoform 2 knockout, 7 weeks following gene deletion
SLRP	Small leucine-rich proteoglycan
TGF-β	Transforming growth factor-β
TIMP	Tissue inhibitor metalloproteinase

TLR	Toll-like receptor
TNF-α	Tumor necrosis factor-α
TUNEL	Terminal dUTP nick end labeling
WT	Wild-type

Introduction

Heart failure - general aspects

Definition

Heart failure (HF) has been defined as a clinical syndrome in which patients have symptoms such as breathlessness at rest or with exercise, and/or fatigue, signs of fluid retention (such as pulmonary congestion or ankle swelling) in addition to objective evidence of an abnormality of the structure or function of the heart at rest[1].

Epidemiology

HF is the leading cause of death in developed countries and is the leading cause of hospitalization in elderly patients. The prevalence of HF is according to the European Society of Cardiology between 2 and 3% and rises sharply at ~75 years of age, with prevalence in 70- to 80-year-old people at approximately 10 to 20%[1]. Overall prevalence of HF is increasing due to aging of the population. In the 1997 Rotterdam study, the life time risk of HF for a person at 55 years of age was estimated at 33.0% in men and 28.5% in women[2]. The age-adjusted mortality from HF is falling at least in part due to modern treatment in some countries[3-6]. Unfortunately, despite contemporary medical management, long-time survival rates are poor, and overall 50% of patients are dead 4 years after diagnosis[1].

Aetiology

Coronary heart disease is by far the most common cause of HF, and is the initiating cause in ~70% of the HF patients[5,7]. Cardiac valve disease accounts for 10%, and cardiomyopathies (hypertrophic, dilated, restrictive, arrhythmogenic right ventricular and unclassified cardiomyopathies) for another 10%[1].

Heart failure in children

The most common cause of paediatric HF is congenital cardiac malformations[8], but cardiomyopathies are the most common cause in children with a structurally normal heart. The remarkable improvement in survival of patients with congenital heart disease has led to a continually growing number of grown-up congenital heart disease (GUCH) patients, in particular those with a more complex disease[9]. HF is a frequent problem in the GUCH population. A major difference between adult and paediatric heart disease is that in paediatrics, much of the pathology is due to an abnormal right ventricle (RV), either due to congenital cardiac malformations or pulmonary hypertension. In congenital cardiac malformations, RV function can be affected in several ways. For example, in hypoplastic right heart syndromes, the three parts of the RV do not form normally or may be missing entirely. There may be defects in the interventricular septum, or abnormal left ventricle (LV) function, which in turn affect RV contraction. Volume overload of the RV can arise through

significant pulmonary or tricuspid valve insufficiency. The RV can experience increased afterload if there is right ventricular outflow obstruction at the subpulmonary, pulmonary, or suprapulmonary level, or if it is serving as the systemic ventricle. Depending on the severity of the different causes of RV affliction, cardiac remodelling and HF may occur.

Cardiac remodelling

Definition

Cardiac remodelling is defined as genome expression, molecular, cellular, and interstitial changes that manifest clinically as changes in the size, shape, and function of the heart after cardiac injury[10].

Remodelling of cardiomyocytes

Cardiomyocytes have been the focus of considerable attention in studies of HF and remodelling, given their primary role in heart chamber contraction and their large contribution to the mass of the heart. The key events associated with cellular remodelling of cardiomyocytes are alterations in the contractile apparatus, cell size (hypertrophy), cell shape, and cell survival.

Extracellular matrix remodelling

The extracellular matrix (ECM) in most tissues is composed of a complex arrangement of fibrillar collagen, elastin, proteoglycans, and adhesive proteins such as laminin and fibronectin. A paradigm shift in the understanding of matrix biology is taking place due to the evolving appreciation that the ECM not only provides the structural support for cells but also provides a dynamic microenvironment for cell signalling within the extracellular space[11]. The large number of fibroblasts in the heart serve the primary purpose of synthesizing and regulating the composition of the ECM[12]. Myocardial ECM are largely composed of a complex network of fibrillar collagen[13]. The content and function of myocardial proteoglycans are not well understood, but will be discussed in more detail below.

Collagen network

The most abundant collagen types in the heart (accounting for over 90%) are the type I and type III fibrillar collagens[14]. Type I collagen molecules assemble into thick fibres, which convey tensile strength and provide structural support. Type III collagens form a fine network of fibrils. A number of cardiovascular disorders including myocardial infarction (MI), hypertension, and HF are associated with alterations in the levels, type, stability, and organization of fibrillar collagen[15]. Collagen accumulation is a classical response to tissue injury as seen in pressure-overload[16].

Collagen cross-links

In every tissue and organ of the human body, including the heart, collagen fibrils are stabilized by a process of maturation that involves the formation of biochemical cross-links[17]. In general, newly synthesized collagen is deficient in cross-links and relatively compliant, affording limited tensile strength. Through posttranslational processing, biochemical cross-links are eventually established in these fibres, resulting in mature collagen that is dense, thick, and of considerable tensile strength. Reduction in collagen cross-links has been demonstrated in human and experimental dilated cardiomyopathy with LV dilatation[18-20]. Accordingly, the degree of collagen cross-linking may have a greater impact on myocardial remodelling and function than collagen abundance or the ratio of collagen isoforms, but how, when, and why details of collagen cross-linking are not well understood.

Collagen architecture

The three-dimensional architecture of the fibrillar collagen network is complex and appears to be highly regulated. Studies indicate that the normal collagen weave is considerably disrupted and degraded in the failing myocardium, and the fibres become less frequent and reduced in thickness[21]. The orientation and spatial organization of cells within the ECM may critically influence cellular responses to regulatory signals, such as those induced during cardiac remodelling and failure.

MMPs and matrix remodelling: key concepts

Matrix metalloproteinases (MMPs) are members of an enzyme family that can catalyse the normal turnover of ECM macromolecules such as collagens and proteoglycans (i.e. decorin, biglycan, fibromodulin and lumican). In the myocardium, both fibroblasts and mast cells are believed to synthesize and secrete the majority of the MMPs into the extracellular space[22,23]. MMP expression and activity are elevated in failing hearts of diverse aetiology, suggesting that matrix remodelling by MMPs is a common response of the myocardium to tissue injury[22-25]. For example, MMP-9 may be particularly relevant to the HF process, as it is consistently expressed and activated in human failing myocardium[22-27]. In summary, MMPs disrupt the composition and organization of the ECM in the failing heart, and in so doing, trigger progressive LV dilatation, thinning of the ventricular walls, and cardiac dysfunction.

Regulation of MMP activity

A number of processes regulate the balance of MMP activity including MMP expression and secretion into the ECM, activation of latent MMPs to bioactive forms, and competitive inhibition of activated MMPs by endogenous inhibitors[28]. At the level of MMP gene expression and secretion into the ECM, cytokines and other growth factors that are known to be increased in the failing heart have also been

identified as important physiological MMP gene inducers[25]. The effects of proinflammatory cytokines on ECM homeostasis via MMP expression and activity represent a possible mechanism for the cytokine hypothesis of remodelling and failure. Beyond their effects on matrix metabolism, MMPs are capable of modulating inflammatory pathways by processing cytokines, chemokines and growth factors[29]. MMP-mediated proteolysis may inactivate a chemokine, generate antagonistic derivatives capable of binding to a chemokine receptor without inducing a chemotactic response, or may result in formation of a truncated chemokine with more potent activity[30]. In addition, MMPs may interfere with chemokine binding to glycosaminoglycans, a molecular step that is critical for chemotactic effects[31].

TIMPs: overview and key concepts

An exciting development in the study of MMP biology was the discovery of a family of four inhibitors of MMPs known as the tissue inhibitor metalloproteinases (TIMPs). These metalloproteinases bind to activated MMPs and form 1:1 enzyme–inhibitor complexes that completely prevent the ability of MMPs to degrade substrates. A disruption in the balance of TIMPs relative to MMPs has been documented in association with the pathological turnover of ECM components in cardiovascular disease[32].

Proteoglycans

The basic proteoglycan unit consists of a core protein with one or more covalently attached glycosaminoglycan (GAG) chain(s). Proteoglycans are a major component of the ECM, the filler substance existing between cells in an organism. In the ECM, proteoglycans form large complexes, both to other proteoglycans, hyaluronan and fibrous matrix proteins (such as collagen). Proteoglycans are also involved in binding cations (i.e. sodium, potassium and calcium) and water, and also in the regulation of movement of molecules through the matrix. They can also affect the activity and stability of proteins and signaling molecules within the matrix. Individual functions of proteoglycans can be attributed to either the protein core or the attached GAG chains. Proteoglycans are classified into three major categories: (1) small leucine-rich proteoglycans (SLRPs), (2) modular proteoglycans, and (3) cell-surface proteoglycans[33].

Small leucine-rich proteoglycans

SLRPs are so named for their small size (up to 42kD) and leucine-rich repeats (LRRs) of the core protein[33]. Recently, five distinct classes of SLRPs have been proposed based on shared biological activity and functions[34]. SLRP biology and function are complicated by their post-translational modifications including substitutions with glycosaminoglycan side chains of various types, namely chondroitin sulfate (CS), dermatan sulfate (DS), or keratan sulfate (KS). Over the last two decades, SLRPs have come to be recognized as regulators of collagen fibril

assembly, the strongest evidence being the disorganized collagen fibrils reported in decorin, fibromodulin and lumican null-mice that consequently lose connective tissue function[35,36]. SLRPs are now also recognized as key players in cell signaling, capable of influencing a host of cellular functions such as proliferations, survival, adhesion, migration and inflammatory responses[37]. Further, SLRPs have been shown to modify inflammatory responses through a number of different mechanisms such as activation of the Toll-like receptor (TLR) signaling pathways, binding and sequestering of cytokines and chemokines and interaction with MMPs[38].

Inflammation and heart failure

Cytokine hypothesis

Inflammation is the classical biological response to injury and serves as a principal mechanism for organismal adaptation and tissue repair. In 1990, Levine et al. reported that TNF-α is systemically elevated in patients with HF[39]. Since that time, an overwhelming number of studies have described a primary role for activated proinflammatory cytokines in the disruption of cardiac structure and function associated with the progression of HF[40]. The results of these investigations have prompted the "cytokine hypothesis"[41], raising the possibility that cytokines and other inflammatory mediators may be important targets for HF therapeutics. Despite compelling evidence in animal models, anti-TNF-α approaches in patients with HF have been uniformly unsuccessful[42]. Two large-scale multicentre clinical trials were prematurely halted due to the lack of a demonstrated benefit of anti-TNF-α therapies in patients with HF; in fact, there were concerns that TNF-α blockade may even be harmful. However, Douglas Mann has shown that too large concentrations of the TNF-antagonist etanercept could lead to a pooling-effect and continous relase of the targed cytokine[43]. Such effects might explain the lack of effect in HF patients treated with anti-TNF-α therapies as etanercept. Despite recent studies suggesting positive effects of anti-inflammatory treatment in subgroups of HF patients[44,45], the use of cytokines as therapeutic targets or as markers of cardiac disease is not considered to be a part of current clinical practice. The lack of success in this research field may also be related to the fact that many studies have been performed in heterogeneous patient populations with HF of varying aetiologies[46]. If cytokine activation differs according to the individual aetiology and form of HF, such approaches might not identify the correct targets or markers.

Chemokines

Chemokines are small (8-11 kDa) heparin-binding single polypeptide chemotactic cytokines (ranging from 70 to 100 amino acids). These cytokines are involved in the trafficking of leucocytes and play an important role in the control and regulation of leukocyte homeostasis in normal and diseased tissue. The chemokine superfamily is divided into four groups (CC, CXC, CX3C and XC), according to the two closely paired and highly conserved cysteine residues in their protein sequence[47].

Chemokines induce cell migration and activation by binding to specific G-protein–coupled cell-surface receptors on target cells[48,49]. Four human CXC chemokine receptors (CXCR1 through CXCR4), eight human CC chemokine receptors (CCR1 through CCR8), and one human CXXXC chemokine receptor (CX_3CR1) have been identified. Chemokines also exert diverse biological effects on other cell types such as endothelial cells, fibroblasts, vascular smooth muscle cells, and cardiomyocytes.

CXCL13/CXCR5

CXCL13 (B lymphocyte chemoattractant (BCL)/B-cell attractant chemokine-1 (BCA-1)) are constitutively expressed within secondary lymphoid organs and regulate lymphocyte and dendritic cells homing to these organs[50-52]. CXCL13 is thought to be the only ligand for CXCR5, which was formally known as BLR1[53]. Expression of CXCR5 has been detected on mature recirculating B cells, a small subset of CD4+ and CD8+ T cells, and skin-derived migratory dendritic cells[54-56]. CXCL13 is expressed by follicular dendritic cells and other stromal cells located in the B-cell regions of secondary lymphoid organs[51,57]. CXCR5 is essentially responsible for guiding B cells into B-cell regions of secondary lymphoid organs. However, CXCR5 expression in a subset of T cells strongly suggests a role for this receptor in T-cell migration as well. Thus, while CXCL13 is known to dictate homing and motility of B cells in lymphoid tissue, more recent studies suggest that CXCL13 is also involved in the formation of ectopic lymphoid tissue in chronic inflammation[58]. In line with its newly discovered role in the immune system, CXCL13 has been suggested to be involved in the pathogenesis of rheumatoid arthritis[59], Sjögren syndrome[60-62], inflammatory bowel disease[63], and multiple sclerosis[64].

Chemokines and heart failure

There is growing evidence to suggest that chemokines and their receptors play an important pathogenic role in various cardiovascular disorders and in various forms of myocardial failure[65-67]. In patients, increased serum levels of CXCL1, CXCL5 and CXCL8 have been found in chronic congestive HF resulting from both ischaemic and nonischaemic cardiomyopathy; as would be expected, the highest levels are present in those with the most advanced disease[68]. Further, enhanced expression of CCR2 and CXCR4 has been observed in the failing human myocardium[69]. Our group has recently shown increased levels of the chemokines CXCL16[70] and CX3CL1[71] in experimental and clinical HF. However, the potential mechanism of action for chemokines in HF is far from clear, and it is important to ascertain if these mediators have beneficial or protective effects.

Aims of the study

The aim of this thesis was to analyse the role of cytokines and chemokines in myocardial hypertrophy and HF.

The specific aims of the separate studies were to:

Paper I: To examine alterations in circulating cytokine levels in cardiac disease with different aetiologies and to relate cytokine activation to differences in pathophysiology.

Paper II: To analyse the role of the chemokine CXCL13 and its receptor CXCR5 in cardiac remodelling and development of HF, based on their roles in inflammation and extracellular matrix remodelling.

Paper III:
i) To identify chemokines which are regulated during RV pressure overload.
ii) To ascertain the contribution of these chemokines to myocardial remodelling during RV overload through modulation of SLRPs.

Paper IV: To ascertain the involvement of SLRPs in cardiac remodelling and reverse remodelling in aortic stenosis (AS) and aortic valve replacement, based on their roles in fibrogenesis and inflammation. We sought to analyse the role of the SLRPs, decorin and lumican, and enzymes responsible for synthesis of their glycosaminoglycan (GAG) chains in a well characterised banding-debanding mouse model.

Summary of results

Paper I:

The main findings were:

(1) No increase in circulating levels of cytokines in mice seven days after aortic banding (AB).

(2) In contrast, we found that the levels of four cytokines (IL-1α, IL-6, G-CSF, and monocyte induced by gamma interferon (MIG), also known as CXCL9) were increased after pulmonary banding (PB) compared to sham-operated mice.

(3) In a group of myocardial infarction (MI) mice without HF, there were no alterations in circulating cytokine levels, except for increased IL-18 levels; this effect was even more pronounced in the HF group.

(4) In SERCA2KO mice seven weeks after gene deletion, the levels of 12 cytokines were increased. Similar to findings in PB with HF mice, levels of IL-1α, IL-6, and G-CSF were increased in the SERCA2KO mice. Levels of IL-12p40 were also increased in this group, in contrast to the decreased values seen in all other HF groups examined. IL-2, IL-3, IL-9, IL-10, eotaxin, interferon (IFN)-γ, monocyte chemoattractant protein (MCP)-1, and macrophage inflammatory protein (MIP)-1β also showed increased levels.

Paper II:

The main findings were:

(1) Mice harbouring a systemic knockout of the CXCR5 gene (CXCR5 $^{-/-}$) displayed increased mortality during a follow-up of 80 days after AB.

(2) Following three weeks of AB, CXCR5 $^{-/-}$ developed significant LV dilatation compared to wild type (WT) mice.

(3) Microarray analysis revealed altered expression of several SLRPs that bind to collagen and modulate fibril assembly.

(4) Protein levels of fibromodulin, decorin and lumican (all SLRPs) were significantly reduced in AB CXCR 5$^{-/-}$ compared to AB WT mice.

(5) Electron microscopy revealed loosely packed ECM with individual collagen fibrils and small networks of proteoglycans in AB CXCR5 $^{-/-}$ mice.

(6) The addition of CXCL13 to cultured cardiac fibroblasts enhanced the expression of SLRPs.

(7) In patients with HF, we observed increased myocardial levels of CXCR5 and SLRPs, which was reversed following LV assist device treatment.

Paper III:

The main findings were:

(1) Increased expression of several chemokines in RV following PB.

(2) Enhanced effect of CXCL16, CX3CL1 and CCL5 on mRNA levels of several SLRPs in myocardial fibroblasts.

(3) Increased post-translational modification of decorin and enhanced protein levels of glycosylated lumican in RV following PB.

(4) Enhanced effects of CXCL16, CX3CL1 and CCL5 (only lumican) on protein levels of glycosylated decorin and lumican in myocardial fibroblasts.
(5) Increased plasma levels of CXCL16 in clinical (pulmonary stenosis) and experimental (PB) RV failure.

Paper IV:

The main findings were:
(1) Increased protein levels of glycosylated decorin in the LV of mice after AB, together with increased expression of several CS/DS GAG chain synthesizing enzymes.
(2) A gradual decrease in the glycosylated protein levels of decorin and certain CS/DS GAG synthesizing enzymes (i.e., chondroitin sulfate synthase -1 and -3 (CHSY-1 and -3)) in the LV after DB.
(3) Upregulation of one of these CS/DS enzymes, namely chondroitin polymerising factor (CHPF), in cardiac fibroblasts after CXCL16 stimulation.
(4) Increased protein levels of lumican core protein with N-linked oligosaccharides, in the LV of mice after AB, which were decreased after debanding (DB).

Methodological considerations

Patients and healthy controls

The patients included in Paper II were recruited from the Department of Cardiology at Oslo University Hospital, Rikshospitalet, Oslo, Norway. The aetiology of HF was classified as coronary artery disease or dilated cardiomyopathy based on disease history, echocardiographic examinations and coronary angiographic examinations. All patients had NYHA class IV HF. Eight were male and one was female, and the mean age was 29±5 years. LV tissue was available at the time of implantation and at the time of removal (heart transplantation) of a continuous-flow LV assist device (LVAD; EntrAssist, Ventracor Ltd, Chatswood, Australia). Average time on LVAD was 8.0±1.7 months. Control (non-HF) human LV tissue was obtained from subjects whose hearts were rejected as cardiac donors for surgical reasons (n=5). The cause of death of donors was cerebrovascular accident, and none had a history of heart disease. To keep confounding factors to a minimum, patients with other accompanying conditions known to modulate inflammation (e.g., autoimmune diseases, infections, malignancies, or connective tissue diseases) were excluded from the study. In Paper III, the patients were recruited from the Department of Paediatrics at Oslo University Hospital, Rikshospitalet, Oslo, Norway. Nine patients (4 male, 5 female, mean age 64 months (range, 2-186 months)) were recruited after referral to a tertiary clinic for first-time or follow-up control of moderate to severe pulmonary stenosis. Four of the patients underwent catheterization of the RV for percutaneous balloon pulmonary valvuloplasty (BVP). All patients were evaluated by continuous Doppler echocardiography. Patients with a peak pulmonary valve velocity higher than 3 m/s were included. This cut-off value was chosen because it represents a gradient above which balloon valvuloplasty can be considered. All patients had typical valvular pulmonary stenosis. There were no associated cardiac defects in 8 patients, but one patient had mild supravalvular aortic stenosis with a peak aortic valve velocity amounting to 2.0 m/s. The same patient had Williams syndrome. Two patients had mild to moderate pulmonary regurgitation. None had clinical signs of right ventricular failure. Exclusion criteria included signs of infection at clinical examination and/or serum levels of C-reactive protein (CRP) >10 mg/L. Healthy children of hospital staff (n=4), and a group of children with nevus flammeus without additional chronic illness (n=5) served as control subjects. All controls (mean age 53 months (range, 12-146 months)) had CRP levels <10 mg/L.

Blood sampling for chemokine measurements

One purpose of this thesis was to study cytokine and chemokine levels in plasma from HF patients and children with pulmonary stenosis, as well as in serum from PB, AB and MI mice and controls. Several factors related to blood collection and processing may influence the measured chemokine levels in plasma and serum. Recovery of chemokines in blood samples is known to be reduced over time after blood collection, particularly if the samples are not stored at 4^{o}C before separation[72].

Therefore, in all our experiments, blood samples were immediately immersed on melting ice before processing.

Animal models

The use of mice as experimental animals has several benefits in that they are small, inexpensive, well characterized and able to be genetically modified. Although there are obvious major phenotype differences, such as size, tail, ear, fur and bilateral venae cavae superior, 99% of mouse genes have a detectable human homolog[73]. There are also physiological differences, e.g. basal heart rate, which is about 600-700 bpm in mice[74] and 60-70 bpm in man. Mice, however, are a desirable model for comparative medical research as the mouse genome has been sequenced and transgenic and knockout techniques have been developed[73]. In all papers in this thesis, C57BL/6 mice and genetically modified animals on a C57BL/6 background were used. We used several different experimental models of HF in mice (**Figure 1**): banding and debanding of the ascending aorta, pulmonary artery banding and ligation of the left coronary artery.

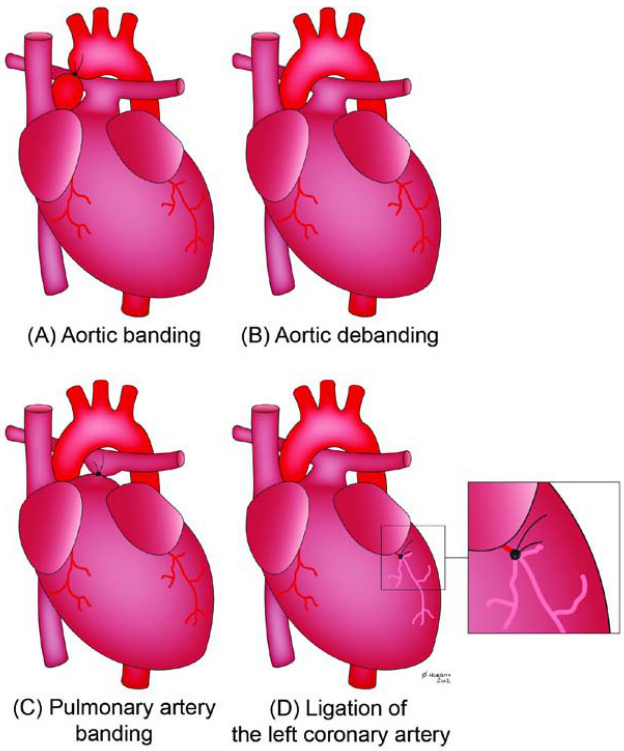

Figure 1. Experimental models of heart failure in mice. ***(A)*** *aortic banding,* ***(B)*** *aortic debanding,* ***(C)*** *pulmonary artery banding,* ***(D)*** *ligation of the left coronary artery.*

Ligation of the left coronary artery and banding of the ascending aorta, are described in detail in Paper I, II and IV and elsewhere[75,76]. The banding-debanding model is described in detail in Paper IV and elsewhere[77,78]. Banding of the pulmonary artery is described in Paper I and elsewhere[74,76]. In Paper I we also used a genetically modified mouse line that develops HF after deletion of the sarco(endo)plasmic reticulum Ca^{2+}-ATPase2 gene induced by tamoxifen treatment, known as the SERCA2KO mice. The generation of SERCA2KO and SERCA2FF (control) mice has been described in detail elsewhere[79]. Mice were euthanised 4 (SERCA2KO4w) and 7 (SERCA2KO7w) weeks after the initiating tamoxifen treatment. The generation of $CXCR5^{-/-}$ mice used in Paper II (C57BL/6 background, now accessible at the Jackson Laboratory, stock number 006659, strain name B6.129S2 (Cg)-*Cxcr5*^{tm1Lipp}/J) has been described in detail elsewhere[80]. For surgical procedures, all animals were anaesthetised and ventilated with a mixture of 2% isoflurane and 98 % oxygen. Most types of anaesthesia will affect cardiac function to a certain degree, rendering the conditions under which the examination is carried out somewhat un-physiological. However, by standardising and optimising the anaesthesia as much as possible, one is at least able to examine relative differences between groups. Since all operations on mice were rather extensive, it is obviously always necessary to compare the responses to sham-operated animals, in order to be able to exclude the effects of the operation itself. Banding of the aorta and the pulmonary artery is achieved rather quickly compared to the natural development of an aortic or pulmonary stenosis, which the procedure is intended to imitate, wheras ligation of the left coronary artery is more comparable to an acute infarction with regard to time-course. However, it may be argued that the pathogenesis is not analogous to that of atherosclerotic coronary disease and MI in humans, given that the mice have otherwise healthy coronary arteries. Nevertheless, the coronary artery ligation and banding models have been shown to be valid models for investigation of myocardial hypertrophy[81].

Echocardiography

Echocardiography is a non-invasive method that can provide serial and detailed information about *in vivo* cardiac function. The method is described in all papers. There are several concerns regarding mouse echocardiography. The collection of echocardiographic recordings requires great skill[82]; of note, all recordings used herein were performed by one operator. In mice, the high heart rate and short working distance represents a technical challenge. We used a fully digital system with modified software that allowed sufficient time resolution for reliable end-systolic and -diastolic measurements. A Q 13 M-Hz linear array transducer designed for the examination of small rodents was also used, giving a sufficiently short working distance. The data were analysed with a VIVID 7 echocardiograph (GE Vingmed Ultrasound, Horten, Norway).

Histology and immunohistochemistry

When interpreting histological and immunohistological sections, one must take into account that these methods are only semiquantitative. Cutting sections as thin as 5 µm is fraught with pitfalls, including folding of the sections, tearing of thin structures and appearance of lines and distortions due to the use of uneven or blunt knives. The methods used for fixation, staining and antibody incubation can also distort the morphology and organization of the tissue to be examined to a certain degree. Staining of sections can be uneven. Finally, the antibodies used for immunohistochemistry can be of varying quality with regard to specificity. All samples were interpreted by two pathologists who were blinded for genotype and intervention.

Transmission electron microscopy

Considering the minute dimensions, slicing of sections is a considerable challenge. The correct interpretation of findings is dependent on considerable experience and knowledge within the field.

Array screening

Microarray screening is a technological development that allows for simultaneous analysis of expression of multiple genes. The Affymetrix Gene Chip analyses over 39,000 transcripts on a single array. The processing of microarray data has been refined and open source software is shared in the scientific community trough BioConductor (http://www.bioconductor.org/). The substantial amount of data generated from microarray screening, however, can be confusing and difficult to interpret. The large number of analyses also represents a statistical concern, as a level of significance of $p=0.05$ just by chance would generate 5 positive tests out of 100 performed. Thus, 39,000 tests would by chance generate 1950 positive tests. There are statistical methods to correct for multiple testing. The false discovery rate (FDR) is the expected rate of false positive results in an analysis of multiple genes, and statistical methods to estimate FDR have been developed and represent important tools in the analysis of microarray data[83]. We have therefore collaborated closely with statistical experts in the field of bioinformatics. The cost of gene chips is rather high, which usually leads to a rather small number of animals included in microarray studies. Important findings must be verified either on the transcriptional level (e.g. by qPCR) or by protein analysis.

RT-qPCR

Real-time quantitative polymerase chain reaction (RT-qPCR) is a method to analyse expression of individual genes by determining levels of mRNA with a particular genetic sequence in a specimen[84-86]. This technique is now widely used to quantify mRNA. Following mRNA isolation, reverse transcriptase is used to create complementary DNA (cDNA), as mRNA is an unstable molecule. As for all methods that require isolation of RNA it is very important to avoid degradation of the material

by immediate snap freezing, as well as repeated freezing and thawing cycles. Treatment with DNase is necessary in order to avoid false DNA signals in the assay. Likewise, varying quality of the RNA obtained can result in false differences in observed amount of PCR product. In our experiments the RNA quality was evaluated using bioanalyser (Agilent) producing a RIN value (RNA Integrity Number). Only samples with high integrity and purity were used in our experiments (absorbance ratio>1.8). A small amount of tissue yields sufficient mRNA to perform multiple RT-qPCR analyses. The accumulation of PCR-product was monitored for each cycle using fluorescent probes (TaqMan). The specificity of primers and probes used is naturally also of great importance. In our experiments we used primers and probes with high specificity, and for comparisons of results obtained from different 96 well plates we made sure to normalize against an endogenous control (RpL4 or GAPDH), which was run on the same plate at the same time. Ideally, the control genes should not be regulated in the tissue or cells investigated, and the interindividual variation should also be low. In our experiments, housekeeping genes and the relative expression were stable between samples within the same experiment.

Western blotting

While analysis of gene expression may be used as a marker of protein synthesis, Western blotting (immunoblotting) is an analytic technique used to determine protein levels[87,88]. Briefly, proteins are isolated from tissue specimens, separated by size using gel electrophoresis, transferred to a membrane and detected using specific antibodies, visualized by chemiluminescence and quantified by densitometry. Membranes were reprobed with actin, vinculin or GAPDH as protein loading controls. Good antibody quality is very important if false negative and false positive results are to be avoided. In the case where the number of samples is so high that they have to be run on two different gels, it is essential to have a sufficient number of the same samples on both gels enabling normalization between the two.

Enzyme linked immunosorbent assays (ELISAs)

Enzyme-linked immunosorbent assay (ELISA) is another technique for protein analysis[72,89]. We have used commercial kits as part of the “sandwich ELISA” technique. Briefly, the kit contains a microplate pre-coated with antibody specific for the protein to be analysed. Standards and samples are applied and unbound substances are washed away. An enzyme-linked protein specific antibody is added to the wells, the plate is washed and a solution with chemical being converted to colour by the enzyme is applied. The intensity of the colour is measured. The intensity of each sample is related to the standard curve, which gives the concentration of the protein of interest in the specimens. Antibody specificity is of course important also in this technique.

Bio-Plex protein assay system based on xMAP technology from Luminex

A Bio-Plex protein assay is a multiplex protein assay that allows for simultaneous examination of multiple proteins in a sample[90]. The technology is based on a family of fluorescently dyed microspheres or beads from Luminex Corp., the use of a special flow cytometer to measure the reactions occurring in the surface of the beads and a high-speed digital signal processor to manage the fluorescent output. Antibody specificity is of high importance in this technique. While proteins are separated by size in Western blot, this is not the case with multiplex and ELISA analysis, thus antibody specificity is even more important for both these techniques than for Western blot.

Isolation and culturing of myocardial-derived cells

Cardiomyocytes and cardiac fibroblasts were isolated from the LV as described by Wollert et al, using tissue digestion and subsequent centrifugation of the cell suspension through a discontinuous Percoll gradient[91]. This procedure yields cardiomyocyte cultures with purity >92% as determined by staining of nuclei and F-actin using Hoechst dye and Oregon Green 488, respectively[92]. Notably, the percentage of cardiomyocytes did not change during the experiments, indicating an absence of proliferative cells in the cultures. Cardiomyocytes and cardiac fibroblasts isolated from immature animals such as neonatal rats are the most commonly used cells for the study of pathological events at a cellular level, such as myocardial hypertrophy and ECM remodeling[93]. Neonatal cells are often preferred over to adult cells for several reasons. First, neonatal cells are easier to culture than the adult type. Adult cardiomyocytes are larger and grow more slowly *in vitro*. Second, when subjected to hypertrophic stimuli, neonatal cells in culture react with characteristic changes in gene expression similar to those found in adult cardiomyocytes *in vivo*. Adult cardiomyocytes and cardiac fibroblasts are derived from terminally differentiated heart tissue, and it is these cells that *in vivo* are subjected to pathogenic stimuli. Therefore, it may be argued that adult cells *in vitro* may be a more accurate model for the *in vivo* situation than neonatal cells. However, although the model has it limitations, neonatal cardiac cells represent a very useful tool for the *in vitro* elucidation of potential pathogenic consequences of over- and underexpression of mediators such as cytokines and chemokines.

General discussion

Cytokine response in cardiac diseases

The aim of Paper I was to examine whether alterations in circulating cytokine levels are dependent on the aetiology of myocardial hypertrophy and HF. The key results in Paper I were that increased serum levels of several cytokines were found in mouse models with increased RV afterload under PB and SERCA2KO7w conditions. In common for PB and SERCA2KO7w conditions was the presence of systemic congestion, suggesting that this is a stimulus for cytokine release into the circulation. Increased cytokine levels associated with systemic congestion indicate the possibility of an extracardiac source of cytokine release. This finding seem to be concordance with the endotoxin hypothesis, which suggests that oedema of the intestines in right-sided HF induces translocation of endotoxins into the systemic circulation[94]. Then, in the bloodstream, endotoxins may activate monocytes to release cytokines, resulting in increased cytokine concentrations[95]. Surprisingly, in mice with pulmonary congestion (AB and MI), several cytokines showed unaltered or even decreased levels in the circulation. Previous studies have shown increased levels of cytokines in heart disease of these aetiologies[68,96,97]. However, the increase in cytokine levels found in such animal and human studies may be caused by systemic congestion following RV failure.

The role of chemokines in cardiac remodelling

Despite the observed enhanced levels of chemokines in experimental and human HF[68-71], the role of chemokines in cardiac remodelling is far from clear. It is of great importance to acknowledge if these mediators have a pathogenic role in the development and progression of HF rather than a beneficial or protective effect. The key results in Paper II were that there was increased mortality and severe LV dilatation in CXCR5-deficient mice in response to LV pressure overload, potentially resulting from ECM alterations that derived from decreased SLRP levels in the myocardium. We found that CXCL13 promotes SLRP expression in cardiac fibroblasts. In Paper III we found that several chemokines upregulated in the pressure-overloaded RV (CXCL16, CX3CL1 and CCL5) also upregulated the expression of SLRPs in cardiac fibroblasts. The same chemokines did also enhance the glycosylated protein levels of decorin and lumican in cardiac fibroblasts medium. In Paper II, III and IV we note the presence of a glycosylated form of decorin, a chondroitin/dermatan sulfate (CS/DS) proteoglycan, with a higher molecular weight in the pressure-overloaded right and left ventricles compared to control mice. In Paper IV we showed that CXCL16 regulates the expression of chondroitin polymerizing enzyme (CHPF), one of the enzymes responsible for CS/DS GAG polymerization.

CXCL13/CXCR5 in cardiac remodelling

Expression of CXCL13-CXCR5 in the heart

Before the present reports, the only reports on CXCL13 or CXCR5 in the heart were in cardiac allografts. Increased CXCL13 expression has been found within the transplanted allograft compared to native hearts, but the source of CXCL13 in the allograft was not known[98]. The same study showed increased expression of CXCR5 on regulatory T cells in the heart. Others have shown features of tertiary lymphoid tissue in cardiac allograft and increased expression of CXCL13-CXCR5 in lymphocytes and macrophages[99]. In Paper II, we showed that both CXCL13 and CXCR5 were expressed in the murine heart. We found significantly increased myocardial expression of CXCR5, but not CXCL13 in AB mice compared to sham operated mice. Within the myocardium, we found mRNA expression of CXCR5 and CXCL13 in cardiomyocytes, fibroblasts and endothelial cells, with the highest expression found in myocardial fibroblasts. Assessment of CXCR5 mRNA levels in myocardial tissue from HF patients showed markedly enhanced gene expression of CXCR5. Production of CXCL13 and CXCR5 in myocardial tissue has, to the best of our knowledge, not previously been demonstrated.

Cardiac phenotype of CXCR5$^{-/-}$ mice following LV pressure-overload

In Paper II, we studied the role of CXCR5 in a knockout model of CXCR5. Others have studied this knockout model and found it viable, but having decreased Payers plaques and lymph nodes[54]. However, the hearts in these mice have never been studied. Our analysis revealed a clear phenotype with significant dilatation and wall thinning of the pressure-overloaded LV. Increased LV volume induces excessive wall stresses that are believed to impair contractile function and trigger maladaptive cardiac remodelling leading to development of overt HF[100]. Increased expression of ANP, BNP and β-MHC genes suggests increased myocardial wall stress in these mice. One working hypothesis of HF is that loss of cardiomyocytes by apoptosis leads to progressive ventricular dysfunction of the heart[101,102]. Myocardial apoptosis may be directly related to progressive wall thinning and failing pump function[103-106]. Apoptosis may play a causative role in the phenotype of LV dilatation and wall thinning of AB CXCR5$^{-/-}$ mice. We did not find any increase in apoptosis using *in situ* TUNEL (Terminal dUTP nick end labeling) analysis. However, quantification of apoptosis is difficult as histochemical visualization of nuclear DNA fragments by TUNEL has limited specificity[101,107]. Ventricular overload can result in myocardial inflammation as demonstrated by myocardial expression of proinflammatory cytokines and leukocyte infiltration into the myocardium[40,108]. As CXCL13 is one of the most potent B-cell chemoattractants[52] and plays an important role in inflammatory diseases[52,109-111], we hypothesized in Paper II that CXCL13 and CXCR5 could also be important in myocardial inflammation. Surprisingly, we did not find any changes in infiltration of CD3 or CD45 positive cells by

immunohistochemistry. However, our data showing a markedly dilated myocardial phenotype in CXCR5 $^{-/-}$ mice exposed to pressure overload, without any significant changes in apoptosis or myocardial leukocyte infiltration, suggest direct involvement of CXCL13/CXCR5 activation on ECM remodelling.

CXCL13/CXCR5 in ECM remodelling

Collagen network in CXCR5 $^{-/-}$ mice following LV pressure-overload

Recently, it has been reported that CXCR5 is involved in remodelling of the ECM in various types of cancer, including colon[112] and prostate cancer[113]. Perhaps the most widely recognized alteration that occurs in the ECM in the failing heart is the development of fibrosis[114]. In Paper II we examined the quality and composition of the collagen in CXCR5 $^{-/-}$ mice following AB. These mice exhibited increased myocardial collagen content following AB compared to WT mice, as illustrated by both Masson trichrome staining and hydroxyproline measurement by HPLC. The deposition of collagen (increased total collagen) is a classical response to tissue injury and an accumulation of myocardial collagen can be seen diffusely in cases of myocardial fibrosis of pressure overload[16,115]. Although we observed increased total collagen content in CXCR5$^{-/-}$ mice, these mice were also characterized by massively disturbed structural frameworks after AB. Electron microscopy revealed loosely packed ECM with individual collagen fibrils in AB CXCR5$^{-/-}$ mice. Other studies indicate that the normal collagen weave is considerably disrupted and degraded in failing myocardium, and that levels of myocardial collagen fibres decrease and the fibres show reduced thickness. For example, in patients with end-stage dilated cardiomyopathy, the collagen network was reduced in parallel to LV dilatation[21].

MMPs in CXCR5 $^{-/-}$ mice following LV pressure-overload

MMPs represent an important family of enzymes capable of degrading the ECM[116]. Enhanced MMP activity and in particular increased activity of MMP-2 and MMP-9, plays an important role in myocardial remodelling, contributing to the development of myocardial failure [117]. The increase in collagen content in CXCR5 $^{-/-}$ mice was accompanied by a significant increase in total MMP activity and gelatinolytic activity of MMP-2 and MMP-9. At the level of MMP gene expression and secretion into the ECM, cytokines and other growth factors that are known to be increased in the failing heart have also been identified as important physiological MMP gene inducers[25]. In particular, proinflammatory cytokines such as TNF-α have been implicated in both MMP expression and the reduction of endogenous inhibitors that leads to overall increases in MMP activity[25,118]. The effects of proinflammatory cytokines on ECM homeostasis via MMP expression and activity describe a possible mechanism by which the cytokine hypothesis of remodelling and failure is viable. Dahl *et al*.[70] have shown that chemokines such as CXCL16 increase MMP activity in myocardial fibroblasts. However, in contrast to what others have shown in prostate cancer cells [113] and in oral squamous cells, [119] we showed in Paper II that CXCL13

decreases total MMP activity in myocardial fibroblasts. The combination of increased collagen content and increased MMP activity suggests enhanced matrix remodelling in CXCR5 $^{-/-}$ mice following AB.

Chemokines in RV remodelling

In studies for Paper I, we found increased circulating levels of several cytokines in models with increased RV afterload, PB and SERCA2KO7w. In Paper III, we identified upregulated chemokines in the RV after pressure-overload. Right-sided HF is a major challenge in the increasing population of adults with congenital heart defects, but few studies have focused on the molecular changes leading to RV failure [120]. While a role for chemokines in LV failure has been established by demonstration of both elevated circulating and myocardial levels in patients with left-sided HF[68-71], little is known about the role of chemokines in right-sided HF. Indeed we found that several chemokines were upregulated in the RV under such conditions. Microarray analysis (Affymetrix) of RV tissue from mice with PB revealed that CXCL10, CXCL6, CX3CL1, CCL5, CXCL16 and CCL2 were the most upregulated chemokines. These findings suggest that the inflammatory system is indeed also involved in development of RV dysfunction.

Potential mechanism of action of chemokines in heart failure

Regulation of SLRPs

Previously, it has been shown that TGF-β induces expression of biglycan, decorin and fibromodulin in different cell systems[121-124]. Also IL4, IL-6 and IL-10 are shown to upregulate decorin expression in human skin fibroblasts[125-127]. Il-1 β and TNF-α have also been implicated in the regulation of decorin synthesis[128]. However, the influence of chemokines on the regulation of SLRPs had not been studied previously. Our findings indicate that chemokines could affect SLRPs synthesis both at a transcriptional level and at a post-translational level.

Chemokines regulate mRNA expression and protein levels of SLRPs

In Paper II, we showed that addition of CXCL13 to cultured cardiac fibroblasts enhanced the expression of SLRPs. In Paper III, we showed that several other chemokines, CXCL16, CX3CL1 and CCL5 increased the expression of the same SLRPs, namely decorin, lumican, biglycan and fibromodulin, by stimulation of cardiac fibroblasts. In the same paper we also showed that CXCL16, CX3CL1 and CCL5 (only lumican) enhanced the glycosylated protein levels of decorin and lumican in myocardial fibroblasts. These studies show, for the first time, that chemokines with increased expression in the heart tissue during pressure-overload can induce mRNA expression and enhance protein levels of SLRPs in cardiac fibroblasts.

Cytokines and chemokines affect SLRPs at a post-translational level

In Paper II, III and IV we found an elongation of the CS/DS GAG chain of decorin after RV and LV pressure-overload. The stimulus for this elongation has not been elucidated. Bassols *et al.*[121] have shown that TGF-β increases the transcription as well as the molecular size of the CS/DS proteoglycans. In Paper IV, we investigated whether chemokines, CXCL16, CX3CL1 and CXCL13, shown to increase decorin expression and protein levels, also could control post-translational modification of the CS/DS GAG chain by regulating CS/DS GAG chain synthesizing enzymes. At least five enzymes generate the CS/DS polysaccharide of decorin, chondroitin polymerizing factor (CHPF)[129], CS synthase (CHSY)-1, -3[130] as well as CS N-acetylgalactosaminyltransferase (CSGALNACT)-1, and -2[131,132]. CHPF, (CHSY)-1, -3 and CSGALNACT-2 were shown to be upregulated in the left pressure-overloaded ventricle, indicating increased glycosylation and elongation of the CS/DS GAG chain of decorin. To the best of our knowledge an increase in these enzymes has never been shown in the pressure-overloaded heart. Interestingly, in Paper IV, after relief of the pressure overload by debanding (DB), CHSY-1 and -3 showed the same reduction in expression as was observed for glycosylated protein levels and the size of the GAG chain. CXCL16 increased the expression of CHPF in cardiac fibroblasts, indicating a possible mechanism for chemokine regulation of CS/DS GAG chain synthesis. However, future studies are required to precisely define the molecular mechanisms behind these effects and to outline the biological consequences.

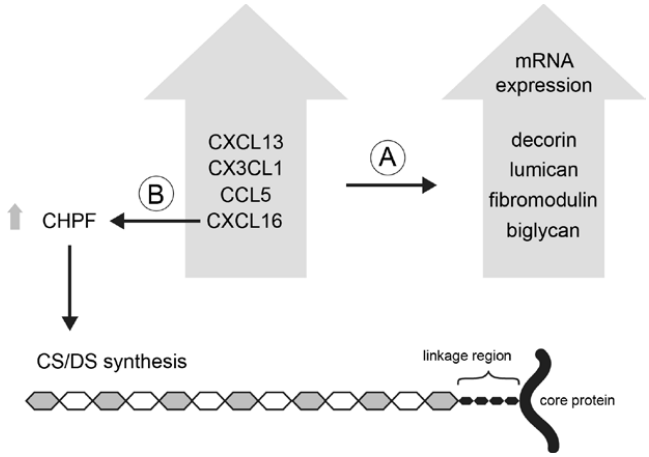

Figure 2. Synthesis of SLRPs is affected at two levels, both at a transcriptional and a post-translational level. (A) *CXCL16, CX3CL1, CCL5 and CXCL13 increase the mRNA exprssion of decorin, lumican, fibromodulin and biglycan.* ***(B)*** *CXCL16 increases the expression of chondroitin polymerizing factor, CHPF, an enzyme important for chondroitin sulfate/dermatan sulfate (CS/DS) synthesis.*

The role of SLRPs in cardiac remodelling

In Paper II, III and IV we found increased protein levels of the SLPRs, decorin and lumican, in pressure-overloaded ventricles. In Paper IV we found a decrease in glycosylated decorin protein levels and lumican core protein with N-linked oligosaccharides after debanding. Together, these findings indicate a role for glycosylated decorin and lumican core protein in myocardial remodelling and reverse remodelling following AB and DB, respectively, which will be discussed in more detail below.

SLRPs as regulators of the collagen network

SLRPs and the collagen network

During the last two decades, SLRPs have been shown to bind collagen and modulate fibril assembly[133]. Disorganized collagen is seen in decorin knockout mice[36]. Null mutations of lumican[81,134] and fibromodulin[135] also lead to abnormal collagen architecture. Collagen fibrils in the ECM in AB CXCR5 $^{-/-}$ mice resemble the structure and organization seen in SLRP knockout mice. Binding of SLRPs to collagen fibrils, regulation of fibril diameter and lateral fusion all seem to be important for the architectural integrity of the collagen network[133]. We do not know at which level the SLRPs act to regulate collagen fibrils. Kalamajski *et al.*[133] suggest that lumican may regulate the intermolecular cross-linking of collagen fibrils. Cross-linking determines the mechanism and level of degradation of collagen fibrils, but no known mechanism for cross-link regulation has been found, except for the enzymatic activity of lysyl oxidase. Kalamajski *et al.*[133] propose that, in the absence of lumican, misalignment of collagen fibrils may appear that in turn could lead to improper or failed cross-linking thereby affecting fibril diameter. Reduction in collagen cross-links has been demonstrated in human dilated cardiomyopathy with LV dilatation[18,20]. In addition, pharmacological inhibition of collagen cross-linking increases myocardial compliance, leading to LV dilatation[136]. Accordingly, the degree of collagen cross-linking may have significant impact on myocardial remodelling.

Role of decorin during pressure-overload

As mentioned previously, in pressure-overloaded RV and LV tissue, Western blotting revealed a glycosylated form of decorin with a higher molecular weight compared to control mice. Changes in the size of the GAG chain of decorin, DS or CS, have been found in a variety of tissues such as skin during wound healing[137] and post-burn hypertrophic scars[138]. Kuwabe *et al.*[139] showed that CS/DS GAG chains oriented orthogonally to collagen fibrils were longer in healing skin than in control skin. Electron microscopy revealed that CS/DS GAG chains were found among tightly packed collagen fibrils in control skin. In contrast, the interfibrillar gaps between each collagen fibril were enlarged in healing skin and elongated CS/DS GAG chains extended from the surface of collagen fibrils across enlarged gaps.

These results suggest that the increase in molecular size of the CS/DS GAG chain is important to the organization of collagen fibrils separated by enlarged interfibrillar gaps in healing skin. It is tempting to speculate that an elongation of the decorin CS/DS GAG chain also increases the distance between collagen fibrils in the pressure-overloaded heart. It is unknown if this is beneficial, to secure the stability and strength of the collagen network during pressure-overload, or in contrast, reducing the strength and forcing a dilatation of the ventricle. However, our studies demonstrate that the size of the GAG chain of decorin is regulated in pressure-overloaded ventricles and reduced to normal size after pressure relief, possibly contributing to the arrangement of collagen fibrils in remodelled cardiac tissue.

SLRPs as signaling molecules and regulators of inflammation

SLRPs and Toll-like receptors

Initially thought to act exclusively as structural components, SLRPs are now recognized as key players in cell signaling and in inflammatory responses[33]. Recently, soluble biglycan has been shown to be a proinflammatory signaling molecule acting as an endogenous ligand of the innate immunity receptors, Toll-like receptors (TLR)-2/4 on macrophages[140,141]. By binding to TLR2 and TLR4, biglycan increases the expression of proinflammatory cytokines such as TNF-α, macrophage inflammatory protein (MIP)-2, MCP-1, RANTES and CXCL13 and pro IL-1β[141-143]. This causes further recruitment of new macrophages, which in turn stimulates production of biglycan, creating a feed-forward cycle that is capable of driving the inflammatory response. Thus, biglycan can boost inflammation by signaling through TLR2 and TLR4. Lumican is involved in the presentation of bacterial lipopolysaccharides to CD14, thereby activating TLR4[144]. Recent clinical and experimental studies suggest that TLRs may play an important role in the development and progression of HF. Frantz *et al.*[145] were the first to report the existence of TLR4 expression in human and rodent hearts. Increased myocardial TLR4 expression was noted in tissue sections from hearts of humans with ischemic cardiomyopathy and of rodents with experimental HF. Using TLR2-deficient mice, Shishido *et al.*[146] reported a significant reduction in mortality and LV dysfunction after coronary artery ligation. These experimental data suggest that TLR 2 and TLR4 may be viable targets for the treatment of HF. The question that remains unanswered is whether it will be possible to modulate the consequences of TLR activation in the heart through blockade of SLRPs (i.e. biglycan and lumican), and what the effects of such interventions during hypertrophy and transition to HF induced by pressure-overload may be.

SLRPs regulate the activity of cytokines and chemokines

Another mechanism whereby SLRPs regulate the inflammatory response in tissues is by interaction with cytokines and chemokines. Decorin, biglycan and fibromodulin

can interact with several cytokines such as TGF-β[147], TNF-α[148], Wnt-1-induced secreted protein 1 (WISP-1)[149] as well as IL-8, a member of the CXC chemokine family[150]. By binding these cytokines, SLRPs can modulate their activity. Furthermore, SLRPs may mediate neutrophil infiltration by forming an immobilized chemokine gradient within inflamed tissues[151].

Effects of SLRPs on TGF-β and MMPs

A great deal of attention has been focused on the antifibrotic properties of decorin as a neutralizing factor affecting TGF-β. We found that TGF-β is markedly increased in both right and left ventricular overload, and decorin might very well have an antifibrotic effect in cardiac remodelling by neutralizing TGF-β activity. Finally, SLRPs may regulate ECM remodelling by modulating MMP activity thereby affecting collagen fibrils. The work by Geng *et al.*[152] demonstrate that the interaction of decorin, fibromodulin and lumican at the surface of either type I or type II collagen fibrils can diminish the susceptibility of the collagen fibrils to both MMP1 and MMP13 cleavage. In the pressure-overload situation, with increased MMP activity, the protective function of SLRPs during stabilization of newly formed collagen fibrils may be of great importance.

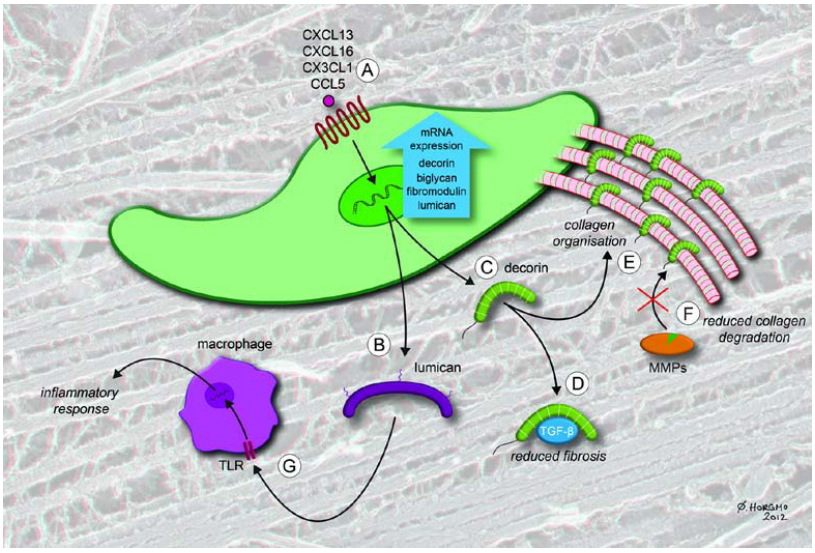

Figure 3. Proposed function of SLRPs in cardiac remodelling during pressure overload. ***(A)*** *CXCL13, CXCL16, CX3CL1 and CCL5 bind to their respective receptors on cardiac fibroblasts and increase mRNA expression of decorin, biglycan, fibromodulin and lumican, and alter the protein levels of* ***(B)*** *lumican and* ***(C)*** *decorin.* ***(D)*** *Decorin is capable of neutralizing the activity of TGF-β, having an antifibrotic effect.* ***(E)*** *Decorin binds to collagen fibrils and helps to stabilize the collagen network and* ***(F)*** *protects the collagen fibrils from cleavage by MMPs.* ***(G)*** *Lumican might activate TLR on machrophages and induce an inflammatory respons.*

Future perspectives

There remain many unanswered questions about the role of chemokines in HF. The possible role of chemokines in cardiac remodelling during pressure-overload is quite intriguing, as are the direct effects stemming from interaction of chemokines with SLRPs. The control of ECM remodelling by chemokines in the failing heart could provide a missing link in our currently inadequate pathophysiological understanding; in addition, a better understanding of the complex role of SLRPs in the normal and failing myocardium may facilitate the development of targeted anti-remodelling strategies. For instance, anti-SLRP treatment may be beneficial in blocking the consequences of TLR activation in the heart. On the other hand, we believe that an increase in the protein level of SLRPs is important for maintenance of normal collagen architecture during pressure-overload. Thus, the question of whether blocking of SLRPs will be beneficial or not remains unanswered. Future goals of our laboratory include further studies on these topics. Knockout mouse models showing overexpression of specific chemokines, such as CXCL16 and CX3CL1, as well as SLRP knockout mice would be extremely valuable to further address the possible role of chemokines and SLRPs in cardiac remodelling.

Conclusions

Paper I:
In conclusion, serum levels of cytokines in mice with heart disease are highly dependent on the aetiology and pathophysiological alterations in the heart and circulation. Increased serum levels of several cytokines were found in models with increased right ventricular afterload, suggesting that systemic congestion is an important stimulus for cytokine release into the circulation in HF.

Paper II:
A lack of CXCR5 leads to LV dilatation and increased mortality during pressure overload, possibly due to the lack of an increase in SLRPs. This study demonstrated a critical role of CXCL13 and CXCR5 in survival and maintenance of cardiac structure in pressure-overload conditions through regulation of proteoglycans essential for correct collagen assembly.

Paper III:
We found that chemokines are upregulated in the pressure-overloaded RV and that CXCL16, CX3CL1 and CCL5 regulate expression and post-translational modification of SLRPs in cardiac fibroblasts. In the pressure-overloaded RV, protein levels of lumican were increased, and a glycosylated form of decorin with a high molecular weight was also present.

Paper IV:
Our findings suggest a role for glycosylated decorin and N-glycosylated lumican core protein in myocardial remodelling and reverse remodelling following AB and DB, respectively. Moreover, several CS/DS GAG chain synthesizing enzymes are upregulated in the pressure-overloaded LV corresponding to the increased levels of glycosylated decorin; notably, levels of two of these enzymes (CHSY-1 and -3) decrease during DB, suggesting a role for these enzymes during reverse remodelling.

Reference list

1 Dickstein, K., Cohen-Solal, A., Filippatos, G., McMurray, J. J., Ponikowski, P., Poole-Wilson, P. A., Stromberg, A., van Veldhuisen, D. J., Atar, D., Hoes, A. W., Keren, A., Mebazaa, A., Nieminen, M., Priori, S. G. & Swedberg, K. ESC guidelines for the diagnosis and treatment of acute and chronic heart failure 2008: the Task Force for the diagnosis and treatment of acute and chronic heart failure 2008 of the European Society of Cardiology. Developed in collaboration with the Heart Failure Association of the ESC (HFA) and endorsed by the European Society of Intensive Care Medicine (ESICM). *Eur.J.Heart Fail.* **10**, 10:933-989 (2008).

2 Bleumink, G. S., Knetsch, A. M., Sturkenboom, M. C., Straus, S. M., Hofman, A., Deckers, J. W., Witteman, J. C. & Stricker, B. H. Quantifying the heart failure epidemic: prevalence, incidence rate, lifetime risk and prognosis of heart failure The Rotterdam Study. *Eur.Heart J.* **25**, 18:1614-1619 (2004).

3 Blackledge, H. M., Tomlinson, J. & Squire, I. B. Prognosis for patients newly admitted to hospital with heart failure: survival trends in 12 220 index admissions in Leicestershire 1993-2001. *Heart* **89**, 6:615-620 (2003).

4 MacIntyre, K., Capewell, S., Stewart, S., Chalmers, J. W., Boyd, J., Finlayson, A., Redpath, A., Pell, J. P. & McMurray, J. J. Evidence of improving prognosis in heart failure: trends in case fatality in 66 547 patients hospitalized between 1986 and 1995. *Circulation* **102**, 10:1126-1131 (2000).

5 Murdoch, D. R., Love, M. P., Robb, S. D., McDonagh, T. A., Davie, A. P., Ford, I., Capewell, S., Morrison, C. E. & McMurray, J. J. Importance of heart failure as a cause of death. Changing contribution to overall mortality and coronary heart disease mortality in Scotland 1979-1992. *Eur.Heart J.* **19**, 12:1829-1835 (1998).

6 Schaufelberger, M., Swedberg, K., Koster, M., Rosen, M. & Rosengren, A. Decreasing one-year mortality and hospitalization rates for heart failure in Sweden; Data from the Swedish Hospital Discharge Registry 1988 to 2000. *Eur.Heart J.* **25**, 4:300-307 (2004).

7 Fox, K. F., Cowie, M. R., Wood, D. A., Coats, A. J., Gibbs, J. S., Underwood, S. R., Turner, R. M., Poole-Wilson, P. A., Davies, S. W. & Sutton, G. C. Coronary artery disease as the cause of incident heart failure in the population. *Eur.Heart J.* **22**, 3:228-236 (2001).

8 Hsu, D. T. & Pearson, G. D. Heart failure in children: part I: history, etiology, and pathophysiology. *Circ.Heart Fail.* **2**, 1:63-70 (2009).

9 Taylor, J. The 2010 version of the ESC guidelines for the management of grown-up adult congenital heart disease are discussed by guidelines task force chairman H. Baumgartner. *Eur.Heart J.* **31**, 23:2825-2826 (2010).

10 Cohn, J. N., Ferrari, R. & Sharpe, N. Cardiac remodeling--concepts and clinical implications: a consensus paper from an international forum on cardiac remodeling. Behalf of an International Forum on Cardiac Remodeling. *J.Am.Coll.Cardiol.* **35**, 3:569-582 (2000).

11 Lukashev, M. E. & Werb, Z. ECM signalling: orchestrating cell behaviour and misbehaviour. *Trends Cell Biol.* **8**, 11:437-441 (1998).

12 Eghbali, M., Czaja, M. J., Zeydel, M., Weiner, F. R., Zern, M. A., Seifter, S. & Blumenfeld, O. O. Collagen chain mRNAs in isolated heart cells from young and adult rats. *J.Mol.Cell Cardiol.* **20**, 3:267-276 (1988).

13 Caulfield, J. B. & Borg, T. K. The collagen network of the heart. *Lab Invest* **40**, 3:364-372 (1979).

14 Weber, K. T., Sun, Y., Tyagi, S. C. & Cleutjens, J. P. Collagen network of the myocardium: function, structural remodeling and regulatory mechanisms. *J.Mol.Cell Cardiol.* **26**, 3:279-292 (1994).

15 Ju, H. & Dixon, I. M. Extracellular matrix and cardiovascular diseases. *Can.J.Cardiol.* **12**, 12:1259-1267 (1996).

16 Swynghedauw, B. Molecular mechanisms of myocardial remodeling. *Physiol Rev.* **79**, 1:215-262 (1999).

17 Reiser, K., McCormick, R. J. & Rucker, R. B. Enzymatic and nonenzymatic cross-linking of collagen and elastin. *FASEB J.* **6**, 7:2439-2449 (1992).

18 Gunja-Smith, Z., Morales, A. R., Romanelli, R. & Woessner, J. F., Jr. Remodeling of human myocardial collagen in idiopathic dilated cardiomyopathy. Role of metalloproteinases and pyridinoline cross-links. *Am.J.Pathol.* **148**, 5:1639-1648 (1996).

19 Spinale, F. G., Zellner, J. L., Johnson, W. S., Eble, D. M. & Munyer, P. D. Cellular and extracellular remodeling with the development and recovery from tachycardia-induced cardiomyopathy: changes in fibrillar collagen, myocyte adhesion capacity and proteoglycans. *J.Mol.Cell Cardiol.* **28**, 8:1591-1608 (1996).

20 Woodiwiss, A. J., Tsotetsi, O. J., Sprott, S., Lancaster, E. J., Mela, T., Chung, E. S., Meyer, T. E. & Norton, G. R. Reduction in myocardial collagen cross-linking parallels left ventricular dilatation in rat models of systolic chamber dysfunction. *Circulation* **103**, 1:155-160 (2001).

21 Weber, K. T., Pick, R., Janicki, J. S., Gadodia, G. & Lakier, J. B. Inadequate collagen tethers in dilated cardiopathy. *Am.Heart J.* **116**, 6 Pt 1:1641-1646 (1988).

22 Brower, G. L., Chancey, A. L., Thanigaraj, S., Matsubara, B. B. & Janicki, J. S. Cause and effect relationship between myocardial mast cell number and matrix metalloproteinase activity. *Am.J.Physiol Heart Circ.Physiol* **283**, 2:H518-H525 (2002).

23 Chancey, A. L., Brower, G. L. & Janicki, J. S. Cardiac mast cell-mediated activation of gelatinase and alteration of ventricular diastolic function. *Am.J.Physiol Heart Circ.Physiol* **282**, 6:H2152-H2158 (2002).

24 Li, Y. Y. & Feldman, A. M. Matrix metalloproteinases in the progression of heart failure: potential therapeutic implications. *Drugs* **61**, 9:1239-1252 (2001).

25 Li, Y. Y., McTiernan, C. F. & Feldman, A. M. Interplay of matrix metalloproteinases, tissue inhibitors of metalloproteinases and their regulators in cardiac matrix remodeling. *Cardiovasc.Res.* **46**, 2:214-224 (2000).

26 Thomas, C. V., Coker, M. L., Zellner, J. L., Handy, J. R., Crumbley, A. J., III & Spinale, F. G. Increased matrix metalloproteinase activity and selective upregulation in LV myocardium from patients with end-stage dilated cardiomyopathy. *Circulation* **97**, 17:1708-1715 (1998).

27 Thompson, M. M. & Squire, I. B. Matrix metalloproteinase-9 expression after myocardial infarction: physiological or pathological? *Cardiovasc.Res.* **54**, 3:495-498 (2002).

28 Mann, D. L. & Spinale, F. G. Activation of matrix metalloproteinases in the failing human heart: breaking the tie that binds. *Circulation* **98**, 17:1699-1702 (1998).

29 Gearing, A. J., Beckett, P., Christodoulou, M., Churchill, M., Clements, J. M., Crimmin, M., Davidson, A. H., Drummond, A. H., Galloway, W. A. & Gilbert, R. Matrix metalloproteinases and processing of pro-TNF-alpha. *J.Leukoc.Biol.* **57**, 5:774-777 (1995).

30 Van, L. P. & Libert, C. Chemokine and cytokine processing by matrix metalloproteinases and its effect on leukocyte migration and inflammation. *J.Leukoc.Biol.* **82**, 6:1375-1381 (2007).

31 Dobaczewski, M., Gonzalez-Quesada, C. & Frangogiannis, N. G. The extracellular matrix as a modulator of the inflammatory and reparative response following myocardial infarction. *J.Mol.Cell Cardiol.* **48**, 3:504-511 (2010).

32 Vanhoutte, D. & Heymans, S. TIMPs and cardiac remodeling: 'Embracing the MMP-independent-side of the family'. *J.Mol.Cell Cardiol.* **48**, 3:445-453 (2010).

33 Schaefer, L. & Schaefer, R. M. Proteoglycans: from structural compounds to signaling molecules. *Cell Tissue Res.* **339**, 1:237-246 (2010).

34 Schaefer, L. & Iozzo, R. V. Biological functions of the small leucine-rich proteoglycans: from genetics to signal transduction. *J.Biol.Chem.* **283**, 31:21305-21309 (2008).

35 Chakravarti, S. Functions of lumican and fibromodulin: lessons from knockout mice. *Glycoconj.J.* **19**, 4-5:287-293 (2002).

36 Danielson, K. G., Baribault, H., Holmes, D. F., Graham, H., Kadler, K. E. & Iozzo, R. V. Targeted disruption of decorin leads to abnormal collagen fibril morphology and skin fragility. *J.Cell Biol.* **136**, 3:729-743 (1997).

37 Iozzo, R. V. & Schaefer, L. Proteoglycans in health and disease: novel regulatory signaling mechanisms evoked by the small leucine-rich proteoglycans. *FEBS J.* **277**, 19:3864-3875 (2010).

38 Gill, S., Wight, T. N. & Frevert, C. W. Proteoglycans: key regulators of pulmonary inflammation and the innate immune response to lung infection. *Anat.Rec.(Hoboken.)* **293**, 6:968-981 (2010).

39 Levine, B., Kalman, J., Mayer, L., Fillit, H. M. & Packer, M. Elevated circulating levels of tumor necrosis factor in severe chronic heart failure. *N.Engl.J.Med.* **323**, 4:236-241 (1990).

40 Mann, D. L. Inflammatory mediators and the failing heart: past, present, and the foreseeable future. *Circ.Res.* **91**, 11:988-998 (2002).

41 Seta, Y., Shan, K., Bozkurt, B., Oral, H. & Mann, D. L. Basic mechanisms in heart failure: the cytokine hypothesis. *J.Card Fail.* **2**, 3:243-249 (1996).

42 Krum, H. Tumor necrosis factor-alpha blockade as a therapeutic strategy in heart failure (RENEWAL and ATTACH): unsuccessful, to be specific. *J.Card Fail.* **8**, 6:365-368 (2002).

43 Mann, D. L., Bozkurt, B., Torre-Amione, G., Soran, O. Z. & Sivasubramanian, N. Effect of the soluble TNF-antagonist etanercept on tumor necrosis factor bioactivity and stability. *Clinical and translational science* **1**, 2:142-145, doi:10.1111/j.1752-8062.2008.00013.x (2008).

44 Gullestad, L., Aass, H., Fjeld, J. G., Wikeby, L., Andreassen, A. K., Ihlen, H., Simonsen, S., Kjekshus, J., Nitter-Hauge, S., Ueland, T., Lien, E., Froland, S. S. & Aukrust, P. Immunomodulating therapy with intravenous immunoglobulin in patients with chronic heart failure. *Circulation* **103**, 2:220-225 (2001).

45 Torre-Amione, G., Anker, S. D., Bourge, R. C., Colucci, W. S., Greenberg, B. H., Hildebrandt, P., Keren, A., Motro, M., Moye, L. A., Otterstad, J. E., Pratt, C. M., Ponikowski, P., Rouleau, J. L., Sestier, F., Winkelmann, B. R. & Young, J. B. Results of a non-specific immunomodulation therapy in chronic heart failure (ACCLAIM trial): a placebo-controlled randomised trial. *Lancet* **371**, 9608:228-236 (2008).

46 Aukrust, P., Ueland, T., Lien, E., Bendtzen, K., Muller, F., Andreassen, A. K., Nordoy, I., Aass, H., Espevik, T., Simonsen, S., Froland, S. S. & Gullestad, L. Cytokine network in congestive heart failure secondary to ischemic or idiopathic dilated cardiomyopathy. *Am.J.Cardiol.* **83**, 3:376-382 (1999).

47 Luster, A. D. Chemokines--chemotactic cytokines that mediate inflammation. *N.Engl.J.Med.* **338**, 7:436-445 (1998).

48 Murphy, P. M. The molecular biology of leukocyte chemoattractant receptors. *Annu.Rev.Immunol.* **12**593-633 (1994).

49 Premack, B. A. & Schall, T. J. Chemokine receptors: gateways to inflammation and infection. *Nat.Med.* **2**, 11:1174-1178 (1996).

50 Cyster, J. G. Chemokines and cell migration in secondary lymphoid organs. *Science* **286**, 5447:2098-2102 (1999).

51 Gunn, M. D., Ngo, V. N., Ansel, K. M., Ekland, E. H., Cyster, J. G. & Williams, L. T. A B-cell-homing chemokine made in lymphoid follicles activates Burkitt's lymphoma receptor-1. *Nature* **391**, 6669:799-803 (1998).

52 Legler, D. F., Loetscher, M., Roos, R. S., Clark-Lewis, I., Baggiolini, M. & Moser, B. B cell-attracting chemokine 1, a human CXC chemokine expressed in lymphoid tissues, selectively attracts B lymphocytes via BLR1/CXCR5. *J.Exp.Med.* **187**, 4:655-660 (1998).

53 Dobner, T., Wolf, I., Emrich, T. & Lipp, M. Differentiation-specific expression of a novel G protein-coupled receptor from Burkitt's lymphoma. *Eur.J.Immunol.* **22**, 11:2795-2799 (1992).

54 Forster, R., Emrich, T., Kremmer, E. & Lipp, M. Expression of the G-protein--coupled receptor BLR1 defines mature, recirculating B cells and a subset of T-helper memory cells. *Blood* **84**, 3:830-840 (1994).

55 Wu, M. T. & Hwang, S. T. CXCR5-transduced bone marrow-derived dendritic cells traffic to B cell zones of lymph nodes and modify antigen-specific immune responses. *J.Immunol.* **168**, 10:5096-5102 (2002).

56 Yu, P., Wang, Y., Chin, R. K., Martinez-Pomares, L., Gordon, S., Kosco-Vibois, M. H., Cyster, J. & Fu, Y. X. B cells control the migration of a subset of dendritic cells into B cell follicles via CXC chemokine ligand 13 in a lymphotoxin-dependent fashion. *J.Immunol.* **168**, 10:5117-5123 (2002).

57 Ansel, K. M., Ngo, V. N., Hyman, P. L., Luther, S. A., Forster, R., Sedgwick, J. D., Browning, J. L., Lipp, M. & Cyster, J. G. A chemokine-driven positive feedback loop organizes lymphoid follicles. *Nature* **406**, 6793:309-314 (2000).

58 Weyand, C. M. & Goronzy, J. J. Ectopic germinal center formation in rheumatoid synovitis. *Annals of the New York Academy of Sciences* **987**140-149 (2003).

59 Shi, K., Hayashida, K., Kaneko, M., Hashimoto, J., Tomita, T., Lipsky, P. E., Yoshikawa, H. & Ochi, T. Lymphoid chemokine B cell-attracting chemokine-1 (CXCL13) is expressed in germinal center of ectopic lymphoid follicles within the synovium of chronic arthritis patients. *J Immunol* **166**, 1:650-655 (2001).

60 Amft, N., Curnow, S. J., Scheel-Toellner, D., Devadas, A., Oates, J., Crocker, J., Hamburger, J., Ainsworth, J., Mathews, J., Salmon, M., Bowman, S. J. &

Buckley, C. D. Ectopic expression of the B cell-attracting chemokine BCA-1 (CXCL13) on endothelial cells and within lymphoid follicles contributes to the establishment of germinal center-like structures in Sjogren's syndrome. *Arthritis and rheumatism* **44**, 11:2633-2641 (2001).

61 Salomonsson, S., Larsson, P., Tengner, P., Mellquist, E., Hjelmstrom, P. & Wahren-Herlenius, M. Expression of the B cell-attracting chemokine CXCL13 in the target organ and autoantibody production in ectopic lymphoid tissue in the chronic inflammatory disease Sjogren's syndrome. *Scandinavian journal of immunology* **55**, 4:336-342 (2002).

62 Xanthou, G., Polihronis, M., Tzioufas, A. G., Paikos, S., Sideras, P. & Moutsopoulos, H. M. "Lymphoid" chemokine messenger RNA expression by epithelial cells in the chronic inflammatory lesion of the salivary glands of Sjogren's syndrome patients: possible participation in lymphoid structure formation. *Arthritis and rheumatism* **44**, 2:408-418, doi:10.1002/1529-0131(200102)44:2<408::AID-ANR60>3.0.CO;2-0 (2001).

63 Carlsen, H. S., Baekkevold, E. S., Johansen, F. E., Haraldsen, G. & Brandtzaeg, P. B cell attracting chemokine 1 (CXCL13) and its receptor CXCR5 are expressed in normal and aberrant gut associated lymphoid tissue. *Gut* **51**, 3:364-371 (2002),1773345.

64 Festa, E. D., Hankiewicz, K., Kim, S., Skurnick, J., Wolansky, L. J., Cook, S. D. & Cadavid, D. Serum levels of CXCL13 are elevated in active multiple sclerosis. *Mult Scler* **15**, 11:1271-1279, doi:10.1177/1352458509107017 (2009).

65 Aukrust, P., Halvorsen, B., Yndestad, A., Ueland, T., Oie, E., Otterdal, K., Gullestad, L. & Damas, J. K. Chemokines and cardiovascular risk. *Arterioscler.Thromb.Vasc.Biol.* **28**, 11:1909-1919 (2008).

66 McNeill, E., Channon, K. M. & Greaves, D. R. Inflammatory cell recruitment in cardiovascular disease: murine models and potential clinical applications. *Clin.Sci.(Lond)* **118**, 11:641-655 (2010).

67 Sasayama, S., Okada, M. & Matsumori, A. Chemokines and cardiovascular diseases. *Cardiovasc.Res.* **45**, 2:267-269 (2000).

68 Aukrust, P., Ueland, T., Muller, F., Andreassen, A. K., Nordoy, I., Aas, H., Kjekshus, J., Simonsen, S., Froland, S. S. & Gullestad, L. Elevated circulating levels of C-C chemokines in patients with congestive heart failure. *Circulation* **97**, 12:1136-1143 (1998).

69 Damas, J. K., Eiken, H. G., Oie, E., Bjerkeli, V., Yndestad, A., Ueland, T., Tonnessen, T., Geiran, O. R., Aass, H., Simonsen, S., Christensen, G., Froland, S. S., Attramadal, H., Gullestad, L. & Aukrust, P. Myocardial expression of CC- and CXC-chemokines and their receptors in human end-stage heart failure. *Cardiovasc.Res.* **47**, 4:778-787 (2000).

70 Dahl, C. P., Husberg, C., Gullestad, L., Waehre, A., Damas, J. K., Vinge, L. E., Finsen, A. V., Ueland, T., Florholmen, G., Aakhus, S., Halvorsen, B.,

Aukrust, P., Oie, E., Yndestad, A. & Christensen, G. Increased production of CXCL16 in experimental and clinical heart failure: a possible role in extracellular matrix remodeling. *Circ.Heart Fail.* **2**, 6:624-632 (2009).

71 Husberg, C., Nygard, S., Finsen, A. V., Damas, J. K., Frigessi, A., Oie, E., Waehre, A., Gullestad, L., Aukrust, P., Yndestad, A. & Christensen, G. Cytokine expression profiling of the myocardium reveals a role for CX3CL1 (fractalkine) in heart failure. *J.Mol.Cell Cardiol.* **45**, 2:261-269 (2008).

72 Lequin, R. M. Enzyme immunoassay (EIA)/enzyme-linked immunosorbent assay (ELISA). *Clin.Chem.* **51**, 12:2415-2418 (2005).

73 Waterston, R. H., Lindblad-Toh, K., Birney, E., Rogers, J., Abril, J. F., Agarwal, P., Agarwala, R., Ainscough, R., Alexandersson, M., An, P., Antonarakis, S. E., Attwood, J., Baertsch, R., Bailey, J., Barlow, K., Beck, S., Berry, E., Birren, B., Bloom, T., Bork, P., Botcherby, M., Bray, N., Brent, M. R., Brown, D. G., Brown, S. D., Bult, C., Burton, J., Butler, J., Campbell, R. D., Carninci, P., Cawley, S., Chiaromonte, F., Chinwalla, A. T., Church, D. M., Clamp, M., Clee, C., Collins, F. S., Cook, L. L., Copley, R. R., Coulson, A., Couronne, O., Cuff, J., Curwen, V., Cutts, T., Daly, M., David, R., Davies, J., Delehaunty, K. D., Deri, J., Dermitzakis, E. T., Dewey, C., Dickens, N. J., Diekhans, M., Dodge, S., Dubchak, I., Dunn, D. M., Eddy, S. R., Elnitski, L., Emes, R. D., Eswara, P., Eyras, E., Felsenfeld, A., Fewell, G. A., Flicek, P., Foley, K., Frankel, W. N., Fulton, L. A., Fulton, R. S., Furey, T. S., Gage, D., Gibbs, R. A., Glusman, G., Gnerre, S., Goldman, N., Goodstadt, L., Grafham, D., Graves, T. A., Green, E. D., Gregory, S., Guigo, R., Guyer, M., Hardison, R. C., Haussler, D., Hayashizaki, Y., Hillier, L. W., Hinrichs, A., Hlavina, W., Holzer, T., Hsu, F., Hua, A., Hubbard, T., Hunt, A., Jackson, I., Jaffe, D. B., Johnson, L. S., Jones, M., Jones, T. A., Joy, A., Kamal, M., Karlsson, E. K., Karolchik, D., Kasprzyk, A., Kawai, J., Keibler, E., Kells, C., Kent, W. J., Kirby, A., Kolbe, D. L., Korf, I., Kucherlapati, R. S., Kulbokas, E. J., Kulp, D., Landers, T., Leger, J. P., Leonard, S., Letunic, I., Levine, R., Li, J., Li, M., Lloyd, C., Lucas, S., Ma, B., Maglott, D. R., Mardis, E. R., Matthews, L., Mauceli, E., Mayer, J. H., McCarthy, M., McCombie, W. R., McLaren, S., McLay, K., McPherson, J. D., Meldrim, J., Meredith, B., Mesirov, J. P., Miller, W., Miner, T. L., Mongin, E., Montgomery, K. T., Morgan, M., Mott, R., Mullikin, J. C., Muzny, D. M., Nash, W. E., Nelson, J. O., Nhan, M. N., Nicol, R., Ning, Z., Nusbaum, C., O'Connor, M. J., Okazaki, Y., Oliver, K., Overton-Larty, E., Pachter, L., Parra, G., Pepin, K. H., Peterson, J., Pevzner, P., Plumb, R., Pohl, C. S., Poliakov, A., Ponce, T. C., Ponting, C. P., Potter, S., Quail, M., Reymond, A., Roe, B. A., Roskin, K. M., Rubin, E. M., Rust, A. G., Santos, R., Sapojnikov, V., Schultz, B., Schultz, J., Schwartz, M. S., Schwartz, S., Scott, C., Seaman, S., Searle, S., Sharpe, T., Sheridan, A., Shownkeen, R., Sims, S., Singer, J. B., Slater, G., Smit, A., Smith, D. R., Spencer, B., Stabenau, A., Stange-Thomann, N., Sugnet, C., Suyama, M., Tesler, G., Thompson, J., Torrents, D., Trevaskis, E., Tromp, J., Ucla, C., Ureta-Vidal, A., Vinson, J. P., Von Niederhausern, A. C., Wade, C. M., Wall, M., Weber, R. J., Weiss, R. B., Wendl, M. C., West, A. P., Wetterstrand, K., Wheeler, R., Whelan, S., Wierzbowski, J., Willey, D., Williams, S., Wilson, R. K., Winter, E., Worley, K. C., Wyman, D., Yang, S., Yang, S. P., Zdobnov, E. M., Zody, M. C. &

Lander, E. S. Initial sequencing and comparative analysis of the mouse genome. *Nature* **420**, 6915:520-562 (2002).

74 Rockman, H. A., Ono, S., Ross, R. S., Jones, L. R., Karimi, M., Bhargava, V., Ross, J., Jr. & Chien, K. R. Molecular and physiological alterations in murine ventricular dysfunction. *Proc.Natl.Acad.Sci.U.S.A* **91**, 7:2694-2698 (1994).

75 Iversen, P. O., Woldbaek, P. R., Tonnessen, T. & Christensen, G. Decreased hematopoiesis in bone marrow of mice with congestive heart failure. *Am.J.Physiol Regul.Integr.Comp Physiol* **282**, 1:R166-R172 (2002).

76 Tarnavski, O. Mouse surgical models in cardiovascular research. *Methods Mol.Biol.* **573**115-137 (2009).

77 Bjornstad, J. L., Sjaastad, I., Nygard, S., Hasic, A., Ahmed, M. S., Attramadal, H., Finsen, A. V., Christensen, G. & Tonnessen, T. Collagen isoform shift during the early phase of reverse left ventricular remodelling after relief of pressure overload. *Eur.Heart J.* **32**, 2:236-245 (2011).

78 Bjornstad, J. L., Skrbic, B., Sjaastad, I., Bjornstad, S., Christensen, G. & Tonnessen, T. A mouse model of reverse cardiac remodelling following banding-debanding of the ascending aorta. *Acta Physiol (Oxf)* (2011).

79 Andersson, K. B., Birkeland, J. A., Finsen, A. V., Louch, W. E., Sjaastad, I., Wang, Y., Chen, J., Molkentin, J. D., Chien, K. R., Sejersted, O. M. & Christensen, G. Moderate heart dysfunction in mice with inducible cardiomyocyte-specific excision of the Serca2 gene. *J.Mol.Cell Cardiol.* **47**, 2:180-187 (2009).

80 Forster, R., Mattis, A. E., Kremmer, E., Wolf, E., Brem, G. & Lipp, M. A putative chemokine receptor, BLR1, directs B cell migration to defined lymphoid organs and specific anatomic compartments of the spleen. *Cell* **87**, 6:1037-1047 (1996).

81 Christensen, G., Wang, Y. & Chien, K. R. Physiological assessment of complex cardiac phenotypes in genetically engineered mice. *Am.J.Physiol* **272**, 6 Pt 2:H2513-H2524 (1997).

82 Finsen, A. V., Christensen, G. & Sjaastad, I. Echocardiographic parameters discriminating myocardial infarction with pulmonary congestion from myocardial infarction without congestion in the mouse. *J.Appl.Physiol* **98**, 2:680-689 (2005).

83 Reiner, A., Yekutieli, D. & Benjamini, Y. Identifying differentially expressed genes using false discovery rate controlling procedures. *Bioinformatics* **19**, 3:368-375 (2003).

84 Heid, C. A., Stevens, J., Livak, K. J. & Williams, P. M. Real time quantitative PCR. *Genome Res.* **6**, 10:986-994 (1996).

85 Nolan, T., Hands, R. E. & Bustin, S. A. Quantification of mRNA using real-time RT-PCR. *Nat.Protoc.* **1**, 3:1559-1582 (2006).

86 VanGuilder, H. D., Vrana, K. E. & Freeman, W. M. Twenty-five years of quantitative PCR for gene expression analysis. *Biotechniques* **44**, 5:619-626 (2008).

87 Burnette, W. N. "Western blotting": electrophoretic transfer of proteins from sodium dodecyl sulfate--polyacrylamide gels to unmodified nitrocellulose and radiographic detection with antibody and radioiodinated protein A. *Anal.Biochem.* **112**, 2:195-203 (1981).

88 Towbin, H., Staehelin, T. & Gordon, J. Electrophoretic transfer of proteins from polyacrylamide gels to nitrocellulose sheets: procedure and some applications. *Proc.Natl.Acad.Sci.U.S.A* **76**, 9:4350-4354 (1979).

89 Engvall, E. & Perlmann, P. Enzyme-linked immunosorbent assay (ELISA). Quantitative assay of immunoglobulin G. *Immunochemistry.* **8**, 9:871-874 (1971).

90 Kofoed, K., Schneider, U. V., Scheel, T., Andersen, O. & Eugen-Olsen, J. Development and validation of a multiplex add-on assay for sepsis biomarkers using xMAP technology. *Clin.Chem.* **52**, 7:1284-1293 (2006).

91 Wollert, K. C., Taga, T., Saito, M., Narazaki, M., Kishimoto, T., Glembotski, C. C., Vernallis, A. B., Heath, J. K., Pennica, D., Wood, W. I. & Chien, K. R. Cardiotrophin-1 activates a distinct form of cardiac muscle cell hypertrophy. Assembly of sarcomeric units in series VIA gp130/leukemia inhibitory factor receptor-dependent pathways. *J.Biol.Chem.* **271**, 16:9535-9545 (1996).

92 Florholmen, G., Andersson, K. B., Yndestad, A., Austbo, B., Henriksen, U. L. & Christensen, G. Leukaemia inhibitory factor alters expression of genes involved in rat cardiomyocyte energy metabolism. *Acta Physiol Scand.* **180**, 2:133-142 (2004).

93 Hefti, M. A., Harder, B. A., Eppenberger, H. M. & Schaub, M. C. Signaling pathways in cardiac myocyte hypertrophy. *J.Mol.Cell Cardiol.* **29**, 11:2873-2892 (1997).

94 Anker, S. D., Egerer, K. R., Volk, H. D., Kox, W. J., Poole-Wilson, P. A. & Coats, A. J. Elevated soluble CD14 receptors and altered cytokines in chronic heart failure. *Am.J.Cardiol.* **79**, 10:1426-1430 (1997).

95 Sandek, A., Bauditz, J., Swidsinski, A., Buhner, S., Weber-Eibel, J., von, H. S., Schroedl, W., Karhausen, T., Doehner, W., Rauchhaus, M., Poole-Wilson, P., Volk, H. D., Lochs, H. & Anker, S. D. Altered intestinal function in patients with chronic heart failure. *J.Am.Coll.Cardiol.* **50**, 16:1561-1569 (2007).

96 Deswal, A., Petersen, N. J., Feldman, A. M., Young, J. B., White, B. G. & Mann, D. L. Cytokines and cytokine receptors in advanced heart failure: an analysis of the cytokine database from the Vesnarinone trial (VEST). *Circulation* **103**, 16:2055-2059 (2001).

97 El-Menyar, A. A. Cytokines and myocardial dysfunction: state of the art. *J.Card Fail.* **14**, 1:61-74 (2008).

98 Lee, B. P., Chen, W., Shi, H., Der, S. D., Forster, R. & Zhang, L. CXCR5/CXCL13 interaction is important for double-negative regulatory T cell homing to cardiac allografts. *J.Immunol.* **176**, 9:5276-5283 (2006).

99 Di Carlo, E., D'Antuono, T., Contento, S., Di, N. M., Ballone, E. & Sorrentino, C. Quilty effect has the features of lymphoid neogenesis and shares CXCL13-CXCR5 pathway with recurrent acute cardiac rejections. *Am.J.Transplant.* **7**, 1:201-210 (2007).

100 Spotnitz, H. M. Macro design, structure, and mechanics of the left ventricle. *J.Thorac.Cardiovasc.Surg.* **119**, 5:1053-1077 (2000).

101 Kang, P. M. & Izumo, S. Apoptosis and heart failure: A critical review of the literature. *Circ.Res.* **86**, 11:1107-1113 (2000).

102 Li, Z., Bing, O. H., Long, X., Robinson, K. G. & Lakatta, E. G. Increased cardiomyocyte apoptosis during the transition to heart failure in the spontaneously hypertensive rat. *Am.J.Physiol* **272**, 5 Pt 2:H2313-H2319 (1997).

103 Lee, W. L., Chen, J. W., Ting, C. T., Ishiwata, T., Lin, S. J., Korc, M. & Wang, P. H. Insulin-like growth factor I improves cardiovascular function and suppresses apoptosis of cardiomyocytes in dilated cardiomyopathy. *Endocrinology* **140**, 10:4831-4840 (1999).

104 Li, Q., Li, B., Wang, X., Leri, A., Jana, K. P., Liu, Y., Kajstura, J., Baserga, R. & Anversa, P. Overexpression of insulin-like growth factor-1 in mice protects from myocyte death after infarction, attenuating ventricular dilation, wall stress, and cardiac hypertrophy. *J.Clin.Invest* **100**, 8:1991-1999 (1997).

105 Schaper, J., Elsasser, A. & Kostin, S. The role of cell death in heart failure. *Circ.Res.* **85**, 9:867-869 (1999).

106 Schaper, J., Lorenz-Meyer, S. & Suzuki, K. The role of apoptosis in dilated cardiomyopathy. *Herz* **24**, 3:219-224 (1999).

107 Kanoh, M., Takemura, G., Misao, J., Hayakawa, Y., Aoyama, T., Nishigaki, K., Noda, T., Fujiwara, T., Fukuda, K., Minatoguchi, S. & Fujiwara, H. Significance of myocytes with positive DNA in situ nick end-labeling (TUNEL) in hearts with dilated cardiomyopathy: not apoptosis but DNA repair. *Circulation* **99**, 21:2757-2764 (1999).

108 Gullestad, L. & Aukrust, P. Review of trials in chronic heart failure showing broad-spectrum anti-inflammatory approaches. *Am.J.Cardiol.* **95**, 11A:17C-23C (2005).

109 Schmutz, C., Hulme, A., Burman, A., Salmon, M., Ashton, B., Buckley, C. & Middleton, J. Chemokine receptors in the rheumatoid synovium: upregulation of CXCR5. *Arthritis Res.Ther.* **7**, 2:R217-R229 (2005).

110 Wengner, A. M., Hopken, U. E., Petrow, P. K., Hartmann, S., Schurigt, U., Brauer, R. & Lipp, M. C. *Arthritis Rheum.* **56**, 10:3271-3283 (2007).

111 Winter, S., Loddenkemper, C., Aebischer, A., Rabel, K., Hoffmann, K., Meyer, T. F., Lipp, M. & Hopken, U. E. The chemokine receptor CXCR5 is pivotal for ectopic mucosa-associated lymphoid tissue neogenesis in chronic Helicobacter pylori-induced inflammation. *J.Mol.Med.(Berl)* **88**, 11:1169-1180 (2010).

112 Meijer, J., Zeelenberg, I. S., Sipos, B. & Roos, E. The CXCR5 chemokine receptor is expressed by carcinoma cells and promotes growth of colon carcinoma in the liver. *Cancer research* **66**, 19:9576-9582, doi:10.1158/0008-5472.CAN-06-1507 (2006).

113 Singh, S., Singh, R., Singh, U. P., Rai, S. N., Novakovic, K. R., Chung, L. W., Didier, P. J., Grizzle, W. E. & Lillard, J. W., Jr. Clinical and biological significance of CXCR5 expressed by prostate cancer specimens and cell lines. *Int.J.Cancer* **125**, 10:2288-2295 (2009).

114 Mann, D. L. & Bristow, M. R. Mechanisms and models in heart failure: the biomechanical model and beyond. *Circulation* **111**, 21:2837-2849 (2005).

115 Weber, K. T., Jalil, J. E., Janicki, J. S. & Pick, R. Myocardial collagen remodeling in pressure overload hypertrophy. A case for interstitial heart disease. *Am.J.Hypertens.* **2**, 12 Pt 1:931-940 (1989).

116 Nagase, H. & Woessner, J. F., Jr. Matrix metalloproteinases. *J.Biol.Chem.* **274**, 31:21491-21494 (1999).

117 Spinale, F. G., Coker, M. L., Bond, B. R. & Zellner, J. L. Myocardial matrix degradation and metalloproteinase activation in the failing heart: a potential therapeutic target. *Cardiovascular research* **46**, 2:225-238 (2000).

118 Spinale, F. G., Coker, M. L., Krombach, S. R., Mukherjee, R., Hallak, H., Houck, W. V., Clair, M. J., Kribbs, S. B., Johnson, L. L., Peterson, J. T. & Zile, M. R. Matrix metalloproteinase inhibition during the development of congestive heart failure : effects on left ventricular dimensions and function. *Circ.Res.* **85**, 4:364-376 (1999).

119 Pandruvada, S. N., Yuvaraj, S., Liu, X., Sundaram, K., Shanmugarajan, S., Ries, W. L., Norris, J. S., London, S. D. & Reddy, S. V. Role of CXC chemokine ligand 13 in oral squamous cell carcinoma associated osteolysis in athymic mice. *Int.J.Cancer* **126**, 10:2319-2329 (2010).

120 Warnes, C. A. Adult congenital heart disease importance of the right ventricle. *Journal of the American College of Cardiology* **54**, 21:1903-1910, doi:10.1016/j.jacc.2009.06.048 (2009).

121 Bassols, A. & Massague, J. Transforming growth factor beta regulates the expression and structure of extracellular matrix chondroitin/dermatan sulfate proteoglycans. *J.Biol.Chem.* **263**, 6:3039-3045 (1988).

122 Burton-Wurster, N., Liu, W., Matthews, G. L., Lust, G., Roughley, P. J., Glant, T. T. & Cs-Szabo, G. TGF beta 1 and biglycan, decorin, and fibromodulin metabolism in canine cartilage. *Osteoarthritis.Cartilage.* **11**, 3:167-176 (2003).

123 Osman, N., Getachew, R., Burch, M., Lancaster, G., Wang, R., Wang, H., Zheng, W. & Little, P. J. TGF-beta stimulates biglycan core protein synthesis but not glycosaminoglycan chain elongation via Akt phosphorylation in vascular smooth muscle. *Growth Factors* **29**, 5:203-210 (2011).

124 Tiede, K., Stoter, K., Petrik, C., Chen, W. B., Ungefroren, H., Kruse, M. L., Stoll, M., Unger, T. & Fischer, J. W. Angiotensin II AT(1)-receptor induces biglycan in neonatal cardiac fibroblasts via autocrine release of TGFbeta in vitro. *Cardiovasc.Res.* **60**, 3:538-546 (2003).

125 Strazynski, M., Eble, J. A., Kresse, H. & Schonherr, E. Interleukin (IL)-6 and IL-10 induce decorin mRNA in endothelial cells, but interaction with fibrillar collagen is essential for its translation. *J.Biol.Chem.* **279**, 20:21266-21270 (2004).

126 Wegrowski, Y., Paltot, V., Gillery, P., Kalis, B., Randoux, A. & Maquart, F. X. Stimulation of sulphated glycosaminoglycan and decorin production in adult dermal fibroblasts by recombinant human interleukin-4. *Biochem.J.* **307 (Pt 3)**673-678 (1995).

127 Yamamoto, T., Eckes, B. & Krieg, T. Effect of interleukin-10 on the gene expression of type I collagen, fibronectin, and decorin in human skin fibroblasts: differential regulation by transforming growth factor-beta and monocyte chemoattractant protein-1. *Biochem.Biophys.Res.Commun.* **281**, 1:200-205 (2001).

128 Tufvesson, E. & Westergren-Thorsson, G. Alteration of proteoglycan synthesis in human lung fibroblasts induced by interleukin-1beta and tumor necrosis factor-alpha. *J.Cell Biochem.* **77**, 2:298-309 (2000).

129 Kitagawa, H., Izumikawa, T., Uyama, T. & Sugahara, K. Molecular cloning of a chondroitin polymerizing factor that cooperates with chondroitin synthase for chondroitin polymerization. *J.Biol.Chem.* **278**, 26:23666-23671 (2003).

130 Kitagawa, H., Uyama, T. & Sugahara, K. Molecular cloning and expression of a human chondroitin synthase. *J.Biol.Chem.* **276**, 42:38721-38726 (2001).

131 Uyama, T., Kitagawa, H., Tamura, J. J. & Sugahara, K. Molecular cloning and expression of human chondroitin N-acetylgalactosaminyltransferase: the key enzyme for chain initiation and elongation of chondroitin/dermatan sulfate on the protein linkage region tetrasaccharide shared by heparin/heparan sulfate. *J.Biol.Chem.* **277**, 11:8841-8846 (2002).

132 Uyama, T., Kitagawa, H., Tanaka, J., Tamura, J., Ogawa, T. & Sugahara, K. Molecular cloning and expression of a second chondroitin N-

acetylgalactosaminyltransferase involved in the initiation and elongation of chondroitin/dermatan sulfate. *J.Biol.Chem.* **278**, 5:3072-3078 (2003).

133 Kalamajski, S. & Oldberg, A. The role of small leucine-rich proteoglycans in collagen fibrillogenesis. *Matrix Biol.* **29**, 4:248-253 (2010).

134 Jepsen, K. J., Wu, F., Peragallo, J. H., Paul, J., Roberts, L., Ezura, Y., Oldberg, A., Birk, D. E. & Chakravarti, S. A syndrome of joint laxity and impaired tendon integrity in lumican- and fibromodulin-deficient mice. *J.Biol.Chem.* **277**, 38:35532-35540 (2002).

135 Svensson, L., Aszodi, A., Reinholt, F. P., Fassler, R., Heinegard, D. & Oldberg, A. Fibromodulin-null mice have abnormal collagen fibrils, tissue organization, and altered lumican deposition in tendon. *J.Biol.Chem.* **274**, 14:9636-9647 (1999).

136 Kato, S., Spinale, F. G., Tanaka, R., Johnson, W., Cooper, G. & Zile, M. R. Inhibition of collagen cross-linking: effects on fibrillar collagen and ventricular diastolic function. *Am.J.Physiol* **269**, 3 Pt 2:H863-H868 (1995).

137 Yeo, T. K., Brown, L. & Dvorak, H. F. Alterations in proteoglycan synthesis common to healing wounds and tumors. *Am.J.Pathol.* **138**, 6:1437-1450 (1991).

138 Garg, H. G., Siebert, J. W., Garg, A. & Neame, P. J. Iduronic acid-rich proteoglycans (PGIdoA) and human post-burn scar maturation: isolation and characterization. *Carbohydr.Res.* **267**, 1:105-113 (1995).

139 Kuwaba, K., Kobayashi, M., Nomura, Y., Irie, S. & Koyama, Y. Size control of decorin dermatan sulfate during remodeling of collagen fibrils in healing skin. *J.Dermatol.Sci.* **29**, 3:185-194 (2002).

140 Schaefer, L. Extracellular matrix molecules: endogenous danger signals as new drug targets in kidney diseases. *Curr.Opin.Pharmacol.* **10**, 2:185-190 (2010).

141 Schaefer, L., Babelova, A., Kiss, E., Hausser, H. J., Baliova, M., Krzyzankova, M., Marsche, G., Young, M. F., Mihalik, D., Gotte, M., Malle, E., Schaefer, R. M. & Grone, H. J. The matrix component biglycan is proinflammatory and signals through Toll-like receptors 4 and 2 in macrophages. *J.Clin.Invest* **115**, 8:2223-2233 (2005).

142 Babelova, A., Moreth, K., Tsalastra-Greul, W., Zeng-Brouwers, J., Eickelberg, O., Young, M. F., Bruckner, P., Pfeilschifter, J., Schaefer, R. M., Grone, H. J. & Schaefer, L. Biglycan, a danger signal that activates the NLRP3 inflammasome via toll-like and P2X receptors. *J.Biol.Chem.* **284**, 36:24035-24048 (2009).

143 Moreth, K., Brodbeck, R., Babelova, A., Gretz, N., Spieker, T., Zeng-Brouwers, J., Pfeilschifter, J., Young, M. F., Schaefer, R. M. & Schaefer, L. The proteoglycan biglycan regulates expression of the B cell chemoattractant

CXCL13 and aggravates murine lupus nephritis. *J.Clin.Invest* **120**, 12:4251-4272 (2010).

144 Wu, F., Vij, N., Roberts, L., Lopez-Briones, S., Joyce, S. & Chakravarti, S. A novel role of the lumican core protein in bacterial lipopolysaccharide-induced innate immune response. *J.Biol.Chem.* **282**, 36:26409-26417 (2007).

145 Frantz, S., Kobzik, L., Kim, Y. D., Fukazawa, R., Medzhitov, R., Lee, R. T. & Kelly, R. A. Toll4 (TLR4) expression in cardiac myocytes in normal and failing myocardium. *J.Clin.Invest* **104**, 3:271-280 (1999).

146 Shishido, T., Nozaki, N., Yamaguchi, S., Shibata, Y., Nitobe, J., Miyamoto, T., Takahashi, H., Arimoto, T., Maeda, K., Yamakawa, M., Takeuchi, O., Akira, S., Takeishi, Y. & Kubota, I. Toll-like receptor-2 modulates ventricular remodeling after myocardial infarction. *Circulation* **108**, 23:2905-2910 (2003).

147 Hildebrand, A., Romaris, M., Rasmussen, L. M., Heinegard, D., Twardzik, D. R., Border, W. A. & Ruoslahti, E. Interaction of the small interstitial proteoglycans biglycan, decorin and fibromodulin with transforming growth factor beta. *Biochem.J.* **302 (Pt 2)**527-534 (1994).

148 Tufvesson, E. & Westergren-Thorsson, G. Tumour necrosis factor-alpha interacts with biglycan and decorin. *FEBS Lett.* **530**, 1-3:124-128 (2002).

149 Desnoyers, L., Arnott, D. & Pennica, D. WISP-1 binds to decorin and biglycan. *J.Biol.Chem.* **276**, 50:47599-47607 (2001).

150 Frevert, C. W., Kinsella, M. G., Vathanaprida, C., Goodman, R. B., Baskin, D. G., Proudfoot, A., Wells, T. N., Wight, T. N. & Martin, T. R. Binding of interleukin-8 to heparan sulfate and chondroitin sulfate in lung tissue. *Am.J.Respir.Cell Mol.Biol.* **28**, 4:464-472 (2003).

151 Carlson, E. C., Lin, M., Liu, C. Y., Kao, W. W., Perez, V. L. & Pearlman, E. Keratocan and lumican regulate neutrophil infiltration and corneal clarity in lipopolysaccharide-induced keratitis by direct interaction with CXCL1. *J.Biol.Chem.* **282**, 49:35502-35509 (2007).

152 Geng, Y., McQuillan, D. & Roughley, P. J. SLRP interaction can protect collagen fibrils from cleavage by collagenases. *Matrix Biol.* **25**, 8:484-491 (2006).

I

II

OPEN ACCESS Freely available online

PLoS one

Lack of Chemokine Signaling through CXCR5 Causes Increased Mortality, Ventricular Dilatation and Deranged Matrix during Cardiac Pressure Overload

Anne Waehre[1,10,11]*, Bente Halvorsen[2,10☯], Arne Yndestad[2,10☯], Cathrine Husberg[1,11], Ivar Sjaastad[1,5,10,11], Ståle Nygård[1,11,12], Christen P. Dahl[2,4,11], M. Shakil Ahmed[3,10,11], Alexandra V. Finsen[2,4,11], Henrik Reims[6], William E. Louch[1,11], Denise Hilfiker-Kleiner[7], Leif E. Vinge[2,4,11], Borghild Roald[6], Håvard Attramadal[3,10,11], Martin Lipp[8], Lars Gullestad[2,4,10,11], Pål Aukrust[2,9,10], Geir Christensen[1,10,11]

1 Institute for Experimental Medical Research, Oslo University Hospital Ullevål, Oslo, Norway, **2** Research Institute for Internal Medicine, Oslo University Hospital Rikshospitalet, Oslo, Norway, **3** Institute for Surgical Research, Oslo University Hospital Rikshospitalet, Oslo, Norway, **4** Department of Cardiology, Oslo University Hospital Rikshospitalet, Oslo, Norway, **5** Department of Cardiology, Oslo University Hospital Ullevål, Oslo, Norway, **6** Department of Pathology, Oslo University Hospital Ullevål, Oslo, Norway, **7** Department of Cardiology and Angiology, Hanover Medical School, Hanover, Germany, **8** Department of Molecular Tumor Genetics and Immunogenetics, Max-Delbrück-Center for Molecular Medicine, Berlin, Germany, **9** Section of Clinical Immunology and Infectious Diseases, Oslo University Hospital Rikshospitalet, Oslo, Norway, **10** Faculty of Medicine, University of Oslo, Oslo, Norway, **11** Center for Heart Failure Research, University of Oslo, Oslo, Norway, **12** Bioinformatics Core Facility, Institute for Medical Informatics, Oslo University Hospital Rikshospitalet, Oslo, Norway

Abstract

Rationale: Inflammatory mechanisms have been suggested to play a role in the development of heart failure (HF), but a role for chemokines is largely unknown. Based on their role in inflammation and matrix remodeling in other tissues, we hypothesized that CXCL13 and CXCR5 could be involved in cardiac remodeling during HF.

Objective: We sought to analyze the role of the chemokine CXCL13 and its receptor CXCR5 in cardiac pathophysiology leading to HF.

Methods and Results: Mice harboring a systemic knockout of the CXCR5 ($CXCR5^{-/-}$) displayed increased mortality during a follow-up of 80 days after aortic banding (AB). Following three weeks of AB, $CXCR5^{-/-}$ developed significant left ventricular (LV) dilatation compared to wild type (WT) mice. Microarray analysis revealed altered expression of several small leucine-rich proteoglycans (SLRPs) that bind to collagen and modulate fibril assembly. Protein levels of fibromodulin, decorin and lumican (all SLRPs) were significantly reduced in AB $CXCR5^{-/-}$ compared to AB WT mice. Electron microscopy revealed loosely packed extracellular matrix with individual collagen fibers and small networks of proteoglycans in AB $CXCR5^{-/-}$ mice. Addition of CXCL13 to cultured cardiac fibroblasts enhanced the expression of SLRPs. In patients with HF, we observed increased myocardial levels of CXCR5 and SLRPs, which was reversed following LV assist device treatment.

Conclusions: Lack of CXCR5 leads to LV dilatation and increased mortality during pressure overload, possibly via lack of an increase in SLRPs. This study demonstrates a critical role of the chemokine CXCL13 and CXCR5 in survival and maintaining of cardiac structure upon pressure overload, by regulating proteoglycans essential for correct collagen assembly.

Citation: Waehre A, Halvorsen B, Yndestad A, Husberg C, Sjaastad I, et al. (2011) Lack of Chemokine Signaling through CXCR5 Causes Increased Mortality, Ventricular Dilatation and Deranged Matrix during Cardiac Pressure Overload. PLoS ONE 6(4): e18668. doi:10.1371/journal.pone.0018668

Editor: Kathleen A. Kelly, University of California Los Angeles, United States of America

Received September 22, 2010; **Accepted** March 15, 2011; **Published** April 18, 2011

Funding: Norwegian Research Council, Anders Jahre's Fund for the Promotion of Science, Joh. H. Andresen's Medical Fund. The funders had no role in study design, data collection and analysis, decision to publish, or preparation of the manuscript.

Competing Interests: The authors have declared that no competing interests exist.

* E-mail: anne.waehre@medisin.uio.no

☯ These authors contributed equally to this work.

Introduction

Heart failure (HF) is a disorder associated with low-grade immune activation and inflammation, as evidenced by elevated circulating and myocardial levels of inflammatory cytokines, including tumor necrosis factor (TNF)α, interleukin (IL)-1β and IL-18, and chemokines such as monocyte chemoattractant protein (MCP)-1 and fractalkine [1–5]. A range of experimental studies have also suggested a pathogenic role for several of these inflammatory mediators in the development and progression of HF [4,6–8]. However, the role of inflammation in HF remains incompletely understood. Identification of the most important

mediators of the inflammatory pathways involved in the pathogenesis of HF and their mechanism of action are issues that need to be further clarified.

While most chemokines have been linked to inflammatory processes in peripheral tissue, the homeostatic chemokines (i.e., CCL19, CCL21, and CXCL13) and their corresponding receptors (i.e., CCR7 for [CCL19 and CCL21] and CXCR5 for [CXCL13]) have been associated with development and maintenance of secondary lymphoid organs [9–12], as well as the entry of lymphocytes and dendritic cells to secondary lymphoid tissue [13–15]. Recently, however, reports have pointed to a broader role for these homeostatic chemokines, including modulation of inflammatory and anti-inflammatory responses in lymphoid and non-lymphoid tissue. Thus, while CXCL13 was known to dictate homing and motility of B cells in lymphoid tissue, more recent studies suggest that CXCL13 is involved in the formation of ectopic lymphoid tissue in chronic inflammation [16,17]. This chemokine has also been linked to T cell [9,18,19] and monocyte activation [20] and apoptosis [21]. In line with its newly discovered role in the immune system, CXCL13 has been suggested to be involved in the pathogenesis of rheumatoid arthritis [22], Sjögren syndrome [23–25], inflammatory bowel disease [26], and multiple sclerosis [27]. CXCR5 is a G protein-coupled seven transmembrane receptor and belongs to the CXC chemokine receptor family [28]. Recently, CXCR5 has been found to be involved in remodeling of extracellular matrix (ECM) in various types of cancer, including colon [29] and prostate cancer [30]. However, the potential role for CXCL13 and CXCR5 in the pathogenesis of myocardial remodeling has not been studied.

Based on their potential role in inflammation and matrix remodeling, we hypothesized that CXCL13 and its receptor CXCR5 are involved in cardiac remodeling and development of HF. We examined this hypothesis by studying the cardiac morphology, function and molecular alterations in CXCR5 deficient ($CXCR5^{-/-}$) mice exposed to left ventricular (LV) pressure overload induced by aortic banding (AB).

Results

Expression of CXCR5 and CXCL13 in murine hearts

We first examined if the CXCL13/CXCR5 dyad was regulated during AB in mice. Both CXCL13 and CXCR5 were expressed within the murine heart, and as shown in Fig. 1*A* and *B*, we found significantly enhanced myocardial expression of CXCR5, but not of CXCL13, in mice that underwent AB as compared with sham operated mice. Within the myocardium, we found mRNA expression of CXCL13 and CXCR5 in cardiomyocytes, fibroblasts and endothelial cells with the highest expression of both CXCR5 and CXCL13 in myocardial fibroblasts (Fig. 2*A*, *B*).

Survival during LV pressure overload

As depicted in Kaplan-Meier survival curves (Fig. 3), $CXCR5^{-/-}$ mice exhibited significantly higher mortality rates than WT mice during an 80-day follow-up after AB induction. The differences in mortality emerged after 40 days of AB.

Severe LV dilatation in $CXCR5^{-/-}$ mice following pressure overload

To investigate a potential role for CXCR5 in cardiac remodeling and development of HF, we evaluated cardiac morphology and function in WT and $CXCR5^{-/-}$ mice. Two-dimensional and M-mode echocardiography performed in non-operated WT (n = 6) and $CXCR5^{-/-}$ (n = 6) mice showed no significant differences in LV function or dimensions (Table S1). Twenty-one days after AB, echocardiographic assessment showed comparable increases in flow velocities across the banded region of the aorta in the WT and $CXCR5^{-/-}$ groups. However, LV fractional shortening was reduced by 65% in $CXCR5^{-/-}$ mice, but only by 13% in WT (Table S1). The mean LV diastolic dimension was significantly larger and the LV posterior wall thickness was significantly lower in $CXCR5^{-/-}$ mice compared to WT mice at the same time point (Fig. 4*A*, *B*).

$CXCR5^{-/-}$ mice show increased expression of hypertrophy maker genes in response to pressure overload

Despite similar increases in heart weight to tibial length (HW/TL) ratio in both genotypes after AB, $CXCR5^{-/-}$ mice exhibited a more marked increase in expression of ANP (3.3-fold increase), BNP (2.3-fold increase) and β-MHC (2.5-fold increase) than WT (Fig. S1*A–C*). The marked increase in ANP and BNP in $CXCR5^{-/-}$ mice following AB might suggest increased myocardial wall stress in these mice.

$CXCR5^{-/-}$ mice exhibit major alterations in ECM in response to pressure overload

Since alterations in extracellular matrix (ECM) might be responsible for LV dilatation, we examined the quality and composition of the ECM following AB. $CXCR5^{-/-}$ mice exhibited increased myocardial collagen content following AB as compared with WT mice, as illustrated by both Masson trichrome staining (Fig. 5*A*) and hydroxyproline measurement by HPLC (Fig. 5*B*). This increase in collagen content in $CXCR5^{-/-}$ mice

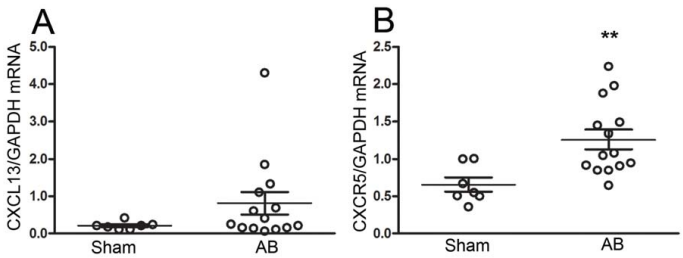

Figure 1. Myocardial gene expression of CXCL13 and CXCR5 in mice. Myocardial gene expression of (**A**) CXCL13 and (**B**) CXCR5 in wild type (WT) Sham (n = 7) and WT aorta banded (AB) (n = 14) group. The results are mean ± SEM. **p<0.01 *vs*. Sham group.
doi:10.1371/journal.pone.0018668.g001

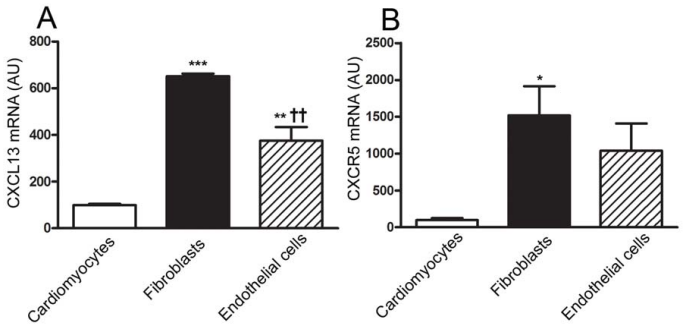

Figure 2. Gene expression of CXCL13 and CXCR5 in myocardial cells in mice. Gene expression of (**A**) CXCL13 and (**B**) CXCR5 in cardiomyocytes, fibroblasts and endothelial cells from wild type mice (n = 3). mRNA levels were assesssed by quantitaive real time PCR. AU = Arbitrary unit. The results are mean ± SEM. * p<0.05, **p<0.01, ***p<0.001 *vs.* cardiomyocytes. ††p <0.01 *vs.* fibroblasts.
doi:10.1371/journal.pone.0018668.g002

was accompanied by a significant increase in total matrix metalloproteinase (MMP) activity (Fig. 5*C*) and gelatinolytic activity (Fig. 5*D, E*). This combination of increased collagen content and increased MMP activity suggest enhanced matrix remodeling in CXCR5 deficient mice following AB.

Microarray analysis identified altered expression of genes encoding non-collagen ECM proteins

In addition to collagen, the quantity and quality of other ECM constituents also importantly influence cardiac function [31]. We therefore performed microarray analysis (Affymetrix) of the myocardium from WT and CXCR5$^{-/-}$ mice 3 weeks after AB. The seeded Bayesian network method [32] was used to explore interactions between differentially expressed genes. This analysis identified a cluster of genes encoding ECM proteins. Interestingly, this cluster contained fibromodulin which belongs to a family of small leucine-rich repeat proteoglycans (SLRPs), which are known to influence ECM assembly [33]. Microarray data are accessible through GEO Series accession number GSE22295 (http://www.ncbi.nlm.nih.gov/geo/query/acc.cgi?acc=GSE22295).

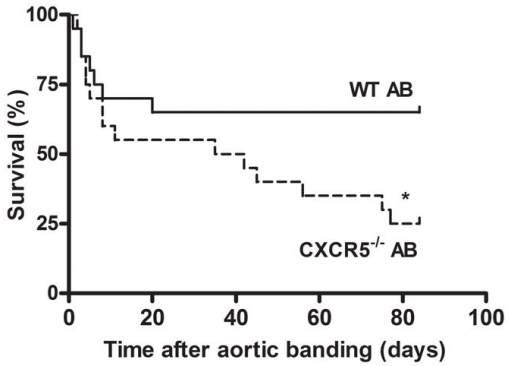

Figure 3. Kaplan-Meier survival curves of wild type (WT) (n = 20) and CXCR5$^{-/-}$ mice (n = 20) after aortic banding (AB). Echocardiographic assessment showed comparable increases in flow velocities across the banded region of the aorta in WT and CXCR5$^{-/-}$ twenty-one days after primary surgery. Differences in survival between WT and CXCR5$^{-/-}$ mice were tested with the log-rank test. *p<0.05 *vs.* WT.
doi:10.1371/journal.pone.0018668.g003

Protein levels of SLRPs following AB in CXCR5$^{-/-}$ and WT mice

To further examine the regulation of SLRPs following AB, we measured protein levels of fibromodulin and other members in the SLRP family, including decorin, lumican and biglycan. With the exception of biglycan, all of these SLRPs were differently regulated in CXCR5 $^{-/-}$ mice compared to WT mice following AB (Fig. 6). While decorin and lumican markedly increased during AB in WT mice, this was not observed in CXCR5$^{-/-}$ mice (Fig. 6*A, B*). Moreover, while fibromodulin decreased following AB in WT and CXCR5 $^{-/-}$ mice, the decrease was significantly more pronounced in the CXCR5$^{-/-}$ mice (Fig. 6*C*).

Electron microscopic analysis revealed loosely packed ECM in CXCR5$^{-/-}$ mice following AB

SLRPs are capable of binding to different types of collagen [34,35], thereby regulating fibril assembly and organization, degradation, and quantitative and functional aspects of the collagen network [33]. To further elucidate the effect of decreased levels of SLRPs during pressure overload, LV tissue sections were examined by electron microscopic analysis in WT and CXCR5-deficient mice. As shown in Fig. 6*D* and *E*, a considerable increase in the extracellular space was observed in LVs from CXCR5$^{-/-}$ as compared to WT mice. In addition, banded WT mice exhibited densely packed collagen fibers of variable thickness and orientation as well as proteoglycan particles associated with fine filaments (Fig. 6*F*). In contrast, the ECM in CXCR5$^{-/-}$ mice exhibited large areas with a coarse network of individual collagen fibrils, and finer networks of proteoglycans with associated filaments (Fig. 6*G*), suggesting deranged ECM.

No difference in apoptosis and leukocyte infiltration between CXCR5$^{-/-}$ and WT mice after pressure overload

CXCL13 has been suggested to exhibit anti-apoptotic properties [36,37]. However, analysis of cardiac apoptosis by *in situ* TUNEL staining revealed that, after either sham-operation or AB, the number of apoptotic cells was similar in WT and CXCR5-deficient mice (Fig. S2). Moreover, although CXCL13 is known to influence lymphocyte trafficking [38,39], we found no significant

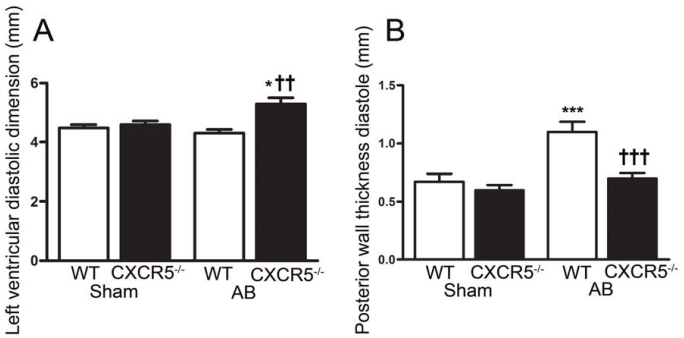

Figure 4. Left ventricular (LV) dilatation in CXCR5$^{-/-}$ mice 3 weeks following aortic banding (AB). LV inner diameter (**A**) and thickness of the posterior wall (**B**) were measured in the wild type (WT) Sham (n = 6), CXCR5$^{-/-}$ Sham (n = 6), WT AB (n = 6), and CXCR5$^{-/-}$ AB (n = 6) groups. The results are mean ± SEM. *p<0.05 and ***p<0.001 *vs.* Sham groups; ††p<0.01 and †††p<0.001 *vs.* WT AB group.
doi:10.1371/journal.pone.0018668.g004

difference in infiltration of CD3$^+$ or CD45$^+$ cells between CXCR5$^{-/-}$ and WT mice after either sham operation or AB (Fig. S3*A* and *B*).

CXCL13 stimulates expression of SLRPs

The changes in ECM in CXCR5$^{-/-}$ mice following AB, consisting of enhanced MMP activity and decreased expression of several SLRPs, could potentially reflect direct effects of CXCL13 on myocardial fibroblasts. In fact, both CXCL13 and CXCR5 were strongly expressed within myocardial fibroblasts, and CXCR5 showed enhanced myocardial expression during AB in WT mice (Fig. 1). In addition, fibroblasts are important producers of ECM proteins, including SLRPs. Stimulation of cardiac neonatal rat fibroblasts with CXCL13 did indeed enhance the expression of fibromodulin, biglycan and lumican, and in particular of decorin, and at the same time down-regulated total MMP activity (Fig. 7*A, B*).

CXCL13-CXCR5 mediate their effects on matrix modulation via ERK1/2 signaling

We next examined alterations in the ERK1/2 pathway in CXCR5$^{-/-}$ following AB, as this pathway is of importance in cardiac remodeling and since CXCL13 signaling through CXCR5 is known to activate the MAPK pathway via ERK 1/2 [40,41]. As shown in Fig. 7*C and D*, LV from CXCR5$^{-/-}$ mice showed decreased levels of phosphorylated ERK1/2 as compared with WT mice. In cardiac fibroblasts, blocking the ERK1/2 pathway by UO126, a highly selective inhibitor of MEK 1 and 2, significantly attenuated up-regulation of fibromodulin following CXCL13 treatment (Fig. 7*E*).

Expression of CXCR5 and SLRPs in patients with HF

Assessments of CXCR5 mRNA levels in myocardial tissue from 9 HF patients (all with advanced HF, NYHA class IV) and 5 controls (non-failing hearts) showed that HF patients had markedly enhanced gene expression of CXCR5 (84% increase, p<0.005). As shown in Fig. 7, the 9 HF patients also had significantly enhanced gene expression of biglycan, lumican and fibromodulin. When the HF patients were treated with continuous-flow LV assist device (LVAD) for 8±1.7 months, improvement in hemodynamic parameters (LV end diastolic volume decreased from 294.9 mL to 237.8 mL, LV diastolic diameter from 7.6 cm to 6.8 cm, and LV end systolic volume from 244.8 mL to 183.4 mL, reflected in an increase in LVEF from 18.2 to 29.6%, p<0.05 for all) was accompanied by a marked decrease in mRNA levels of CXCR5 as well as biglycan and fibromodulin, although the decrease in fibromodulin did not reach statistical significance (Fig. 8).

Discussion

Despite observations of enhanced levels of chemokines and their corresponding receptors in human HF [5,42,43], the role of chemokines in maintaining cardiac structure and function has never been established. The present work clearly demonstrates that the chemokine CXCL13 and its receptor, CXCR5, are critically involved in cardiac remodeling. The key results of this study were increased mortality and severe LV dilatation in CXCR5-deficient mice in response to pressure overload, potentially resulting from impaired quality of ECM. These ECM alterations derived, at least partly from decreased SLRP levels and enhanced MMP activity within the myocardium. Our *in vitro* findings showed that CXCL13 can promote SLRP expression and attenuate MMP activity in myocardial fibroblasts. Therefore, the opposite pattern seen in CXCR5-deficient mice could reflect the inability of their myocardial fibroblasts to respond to CXCL13. These data indicate that the CXCL13/CXCR5 interaction is involved in myocardial remodeling following pressure overload, possibly by regulating proteoglycans crucial for the quality of myocardial ECM. Our findings of a strong expression of CXCL13 and CXCR5 in fibroblasts within murine hearts and enhanced myocardial expression of CXCR5 during AB further support such a notion.

The possible role of chemokines in the pathogenesis of HF has, at least in part, been attributed to the ability of these molecules to promote leukocyte infiltration in failing myocardium. However, in the present study we did not detect altered infiltration of CD3$^+$ and CD45$^+$ cells in CXCR5$^{-/-}$ mice compared to the WT mice following AB. Previously, various chemokines (e.g., CXCL16, MCP-1 and CX3CL1) have been shown to promote direct effects on myocardial fibroblasts and cardiomyocytes *in vitro* [5,43–45]. Also, the lack of CXCR4 has been associated with severe myocardial developmental defects (i.e., ventricular septum defects) [46]. In contrast to CXCR4, CXCR5 deficient mice are viable and display normal morphology and function of the adult heart. However, our present data showing a markedly dilating myocardial phenotype in CXCR5$^{-/-}$ mice exposed to pressure

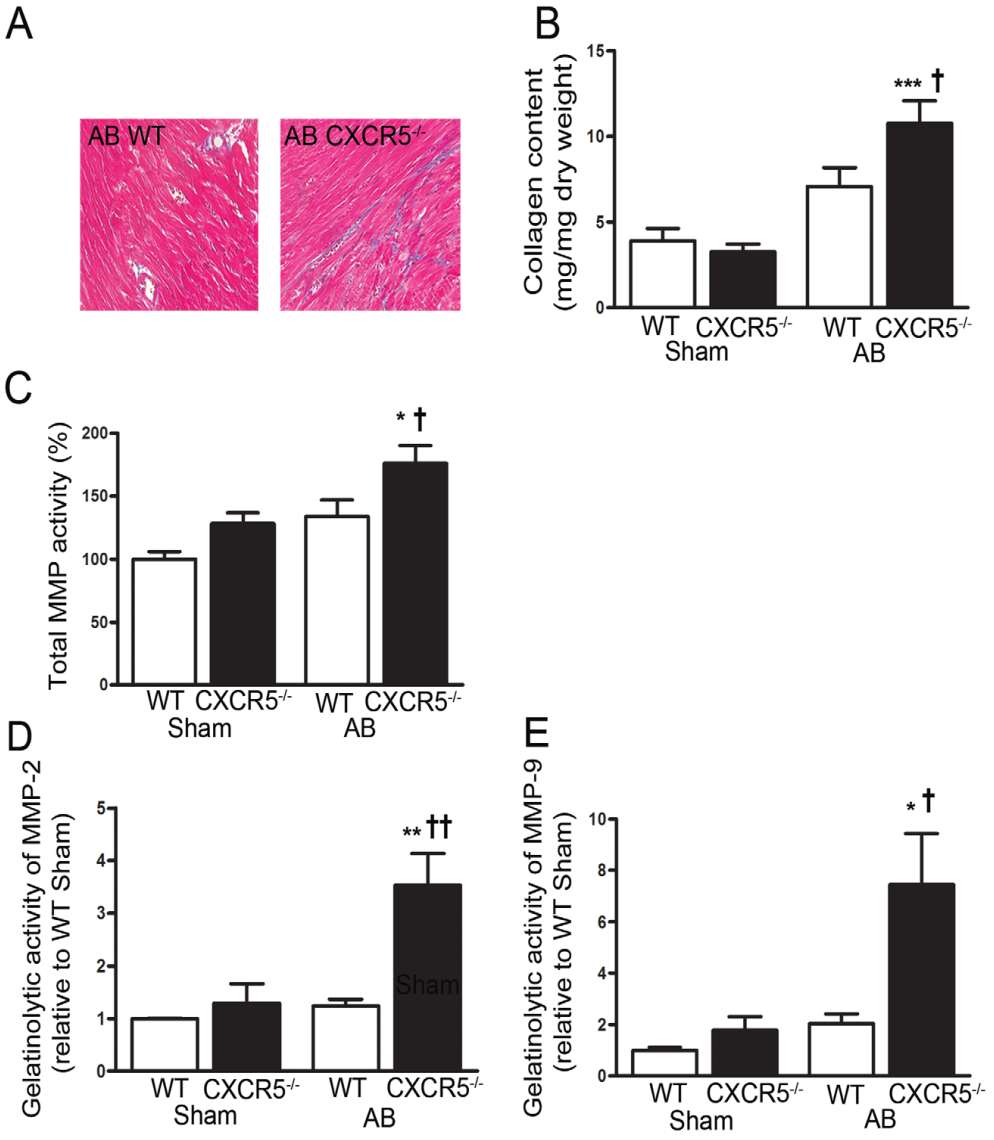

Figure 5. Extracellular matrix remodeling in wild type (WT) and CXCR5$^{-/-}$ mice following aortic banding (AB). Collagen content in myocardium examined with (**A**) Masson trichrome staining in representative sections from AB WT and CXCR5$^{-/-}$ mice and (**B**) by hydroxyproline measurement in WT Sham (n = 13), CXCR5$^{-/-}$ Sham (n = 12), WT AB (n = 13) and CXCR5$^{-/-}$ AB (n = 14) groups. (**C**) Total MMP activity in percentage of the WT Sham group (n = 11) measured in the CXCR5$^{-/-}$ Sham (n = 13), WT AB (n = 9), and CXCR5$^{-/-}$ AB groups (n = 9). (**D**) Gelatinolytic activity of MMP-2 relative to the WT Sham group (n = 5) measured in the CXCR5$^{-/-}$ Sham (n = 5), WT AB (n = 5), and CXCR5$^{-/-}$ AB groups (n = 5) and of (*E*) MMP-9 relative to the WT Sham group (n = 6) measured in the CXCR5$^{-/-}$ Sham (n = 6), WT AB (n = 8), and CXCR5$^{-/-}$ AB groups (n = 9). The results are mean ± SEM. *p<0.05, **p<0.01 and ***p<0.001 *vs.* Sham groups; †p<0.05 and ††p<0.01 *vs.* WT AB groups.
doi:10.1371/journal.pone.0018668.g005

overload, without any significant changes in myocardial leukocyte infiltration, may suggest a direct involvement of CXCL13/CXCR5 activation in myocardial remodeling. The ability of CXCL13 to attenuate MMP activity and increase SLRP expression in myocardial fibroblasts as well as the up-regulation of CXCR5 during AB in WT mice further supports such a notion.

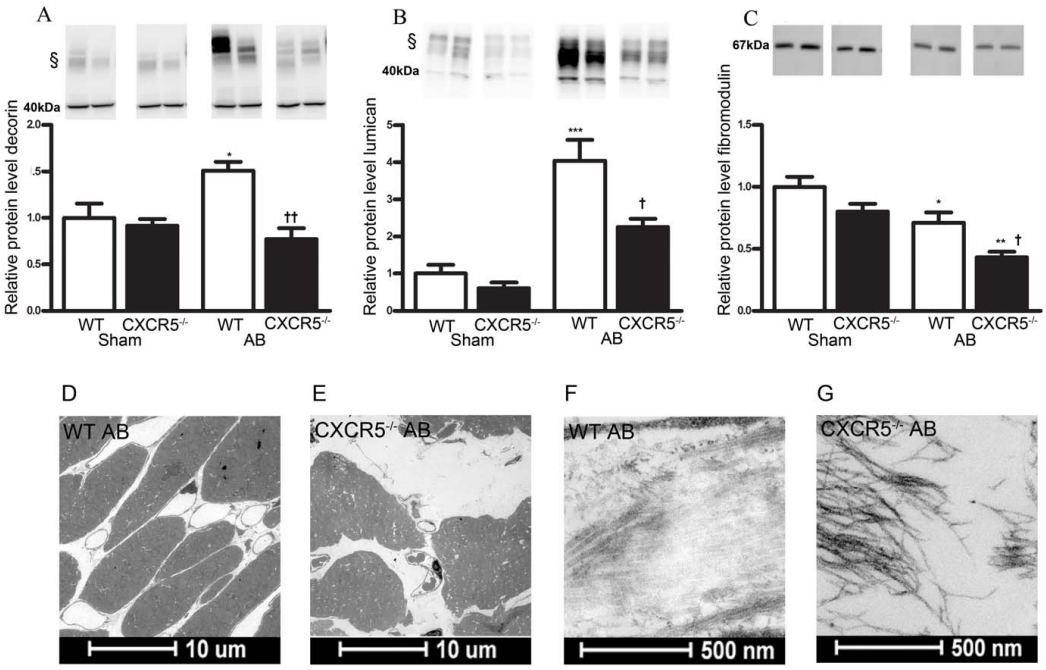

Figure 6. Protein levels of small leucine-rich repeat proteoglycans (SLRPs) and transmission electron microscopic analysis in wild type (WT) and CXCR5$^{-/-}$ mice following aortic banding (AB). Protein levels of (**A**) decorin and (**B**) lumican in (WT) Sham (n = 7), CXCR5$^{-/-}$ Sham (n = 5), WT AB (n = 6), and CXCR5$^{-/-}$ AB (n = 5), and (**C**) fibromodulin in WT Sham (n = 13), CXCR5$^{-/-}$ Sham (n = 12), WT AB (n = 12), and CXCR5$^{-/-}$ AB (n = 11) groups as assessed by western blotting. The upper panels show representative blots from two mice in each group. § Glycosylated forms of decorin and lumican, respectively. The results are mean ± SEM. *p<0.05, **p<0.001 and ***p<0.001 *vs.* Sham groups; †p<0.05 and ††p<0.01 *vs.* WT AB group. The lower panels show representative transmission electron micrographs of the LV free wall at ×440 and ×23000 magnification in WT (**D** and **F**) and CXCR5$^{-/-}$ (**E** and **G**) AB mice.
doi:10.1371/journal.pone.0018668.g006

Collagen synthesis, fibrillogenesis, and matrix degradation must be finely tuned, as an imbalance in these processes might result in cardiac dilatation, cardiac hypertrophy and fibrosis. Although we observed increased total collagen content in CXCR5$^{-/-}$ mice, these mice were also characterized by massively disturbed structural frameworks after AB compared to WT. Our molecular analysis suggested that this distorted ECM structure derives from a failure in the regulation of SLRPs in pressure overloaded CXCR5-deficient mice. SLRPs are known to bind to collagens, and in so doing, regulate the self-assembly process of pro-collagen into fibrils [33–35]. This assembly is necessary for covalent cross-linking which is required for reinforcement of the collagen fibrils. SLRPs have been shown to be up-regulated in the infarcted area in rats and mice following myocardial infarction (MI) [47,48]. Studies in SLRP deficient mice have shown abnormal fibril organization and loose fibril packing in the MI scar [49,50]. In the current study we show an attenuated up-regulation (i.e., decorin and lumican) and a more pronounced decrease (i.e., fibromodulin) in SLRP expression following AB in CXCR5 deficient mice as compared with WT mice. Interestingly, enhanced MMP activity has been found to impair SLRP function [44], and we suggest that the combination of decreased SLRP expression and increased MMP activity could be of major importance for the premature LV dilatation and HF in CXCR5$^{-/-}$ mice following AB.

Our *in vitro* data suggest that CXCL13 via activation of CXCR5 on myocardial fibroblasts induces the expression of SLRPs through the ERK1/2 pathway. This mechanism appears to be absent in fibroblasts from CXCR5$^{-/-}$ mice. ERK is one of the key protein kinases that regulate growth and proliferation of cardiac fibroblasts [40]. In line with a crucial role of CXCL13/CXCR5-mediated ERK1/2 activation for cardiac remodeling in response to pressure overload, ERK1/2 phosphorylation was substantially lower in CXCR5$^{-/-}$ mice compared to WT after AB. These findings further support previous reports of a central role of the ERK pathway for myocardial remodeling [51,52]. In this regard, the present study adds a novel component to this pathway by linking CXCR5-mediated effects to SLRPs and subsequent ECM remodeling.

Our studies in patients with advanced HF suggest that our findings in experimental HF may have relevance to clinical HF. We showed enhanced myocardial expression of CXCR5 and certain SLRPs (i.e., biglycan, lumican and fibromodulin) in the failing myocardium, and notably, biglycan and lumican were down-regulated following the clinical and hemodynamic improvement during treatment with LV assist device. Based on our experimental data, it is tempting to speculate that CXCR5 activation promotes protective responses in ECM in failing myocardium involving enhanced expression of SLRPs. As

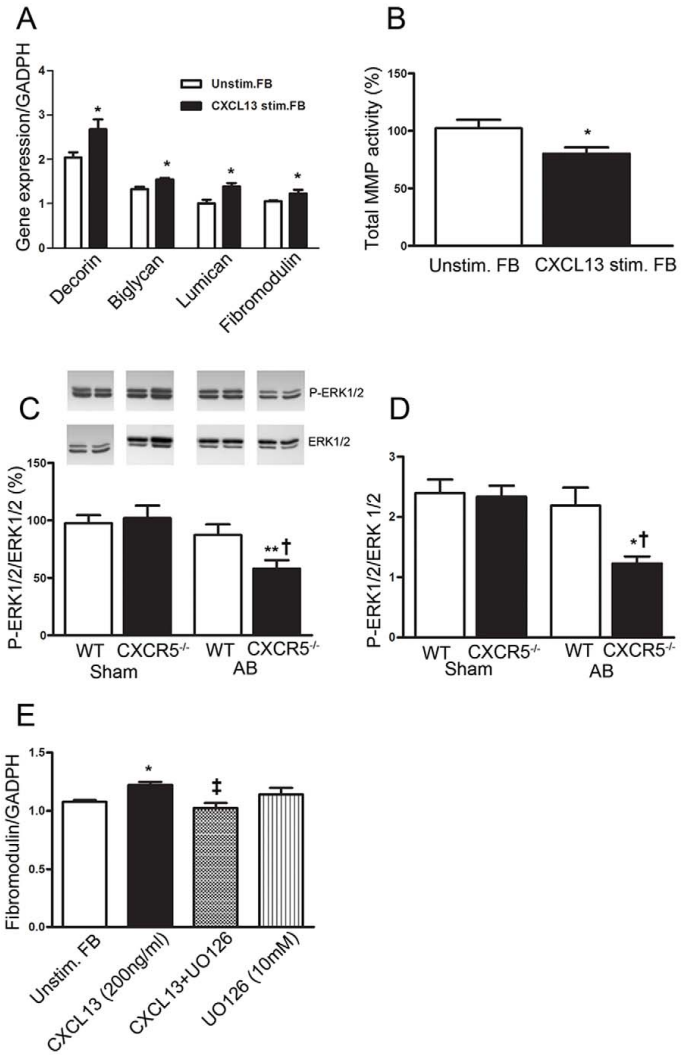

Figure 7. Effects of CXCL13 on gene expression of small leucine-rich repeat proteoglycans (SLRPs), total MMP activity and the intracellular signalling pathway ERK 1/2 in neonatale rat fibroblasts (FB). The effect of CXCL13 (200 ng/ml) stimulation on gene expression of (**A**) decorin, biglycan, lumican and fibromodulin (n = 4) in myocardial FB after 20 hours of stimulation in relation to GAPDH and (**B**) total MMP activity in cell-free supernatant (n = 7) after 20 hours of stimulation. The ratio of phosphorylated ERK 1/2 (p-ERK 1/2) to total ERK 1/2 assessed by (**C**) western blotting in WT Sham (n = 13), CXCR5$^{-/-}$ Sham (n = 12), WT AB (n = 11), and CXCR5$^{-/-}$ AB (n = 10) groups, and by (**D**) BioPlex in WT Sham (n = 6), CXCR5$^{-/-}$ Sham (n = 5), WT AB (n = 7), and CXCR5$^{-/-}$ AB (n = 6) groups. (**E**) The effect of blocking ERK 1/2 activation with UO126 (10 μM) on the CXCL13-mediated induction of fibromodulin gene expression in myocardial FB (n = 4). The results are mean ± SEM. *p<0.05 and **p<0.01 *vs.* unstimulated FB or CXCR5$^{-/-}$ Sham; †p<0.05 *vs*. WT AB group, ‡p<0.05 vs. CXCL13 stimulated FB without inhibitor (UO126).
doi:10.1371/journal.pone.0018668.g007

myocardial function improves, this response is attenuated. At present, however, the stimuli for enhanced myocardial CXCR5 expression in HF and the interpretation of our human data will require further investigation.

In conclusion, we have found that CXCR5 plays an important role in cardiac remodeling during pressure-overload. Loss of CXCR5 in this situation adversely affects matrix remodeling and causes LV dilatation, possibly through altered regulation of proteoglycans crucial for the quality of myocardial ECM (i.e., SLRPs) as well as through enhanced MMP activity. These changes could, at least in part, be attributed to loss of CXCL13 mediated effects on myocardial fibroblasts in CXCR5 deficient mice. The

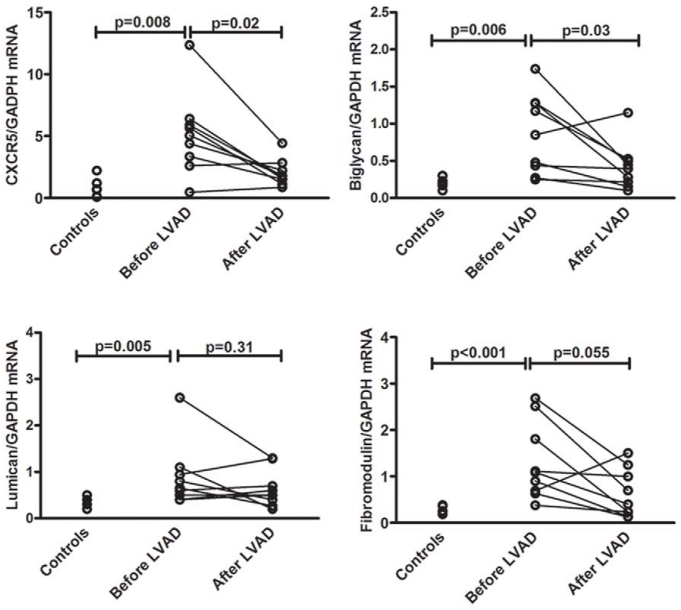

Figure 8. Gene expression of CXCR5, biglycan, lumican and fibromodulin in patients with heart failure (HF) (n = 9) and controls (n = 5) as assesssed by quantitaive real time PCR. In the HF patients, the mRNA levels were measured before and after treatment with continuous-flow left ventricular assist device (LVAD).
doi:10.1371/journal.pone.0018668.g008

identification of molecular and structural changes causing LV dilatation during pressure overload is of major importance for the development of new treatment strategies in HF related to hypertension and aortic stenosis. Future studies should examine how the CXCL13/CXCR5 dyad could be utilized therapeutically in clinical HF.

Materials and Methods

Ethics

All animal experiments were approved by the Norwegian Animal Research Committee (ID 1902) and conform to the Guide for the Care and Use of Laboratory Animals published by the US National Institutes of Health (NIH Publication No. 85–23, revised 1996). The part of the study that involved humans was approved by the local ethics committee (REK Helse Sør-Øst) and conducted according to the ethical guidelines outlined in the Declaration of Helsinki for use of human tissue and subjects. Informed written consent was obtained from all subjects. The authors had full access to the data and take responsibility for its integrity. All authors have read and agree to the manuscript as written.

Data analysis

All data are expressed as group means ± SEM unless indicated otherwise. For comparisons of 2 groups, the Mann-Whitney *U* test was employed. The Wilcoxon test was employed when analysing the effect of LVAD treatment. Differences between the WT Sham, WT AB, CXCR5$^{-/-}$ Sham, and CXCR5$^{-/-}$ AB groups were determined by one-way ANOVA with post-hoc Tukey test. Differences in survival between wild type and CXCR5$^{-/-}$ mice in Fig. 3 were compared using Kaplan- Meier survival curves and tested with the log-rank test. All tests were employed using a 5% significance level.

Animals and AB protocol

Mice were housed in M2 or M3 cages with Bee Kay bedding (Scanbur BK, Nittedal, Norway) in 55% humidity on a 12 h light/dark cycle. Food pellets (RM1, 801151, Scanbur BK) and water were freely available. All mice utilized in this study were male and had a weight 20–30 g. WT C57BL/6 mice were obtained from Taconic (Skensved, Denmark). The generation of CXCR5$^{-/-}$ mice (C57BL/6 background, now accessible at the Jackson Laboratory, stock number 006659, strain name B6.129S2 (Cg)-*Cxcr5*^{tm1Lipp}/J has been described previously [14]. Briefly, gene targeting was performed in 129S2/SvPas-derived D3 embryonic stem cells, replacing the coding region of the CXCR5 gene with a neomycin resistance gene. Mutant mice were backcrossed to C57BL/6 mice for 8 generations. AB was induced in C57BL/6 and CXCR5$^{-/-}$ mice as previously described [53]. Briefly, after being anesthetized with 5% isoflurane and ~98% oxygen in a gas chamber, the animals where endotracheal intubated and the cannula was connected to a volume cycled rodent ventilator (Harvard Apparatus) on supplement of a mixture of ~1.75% isoflurane and ~98% oxygen. A thoracotomy was performed in the second intercostal space on the left side, and the aortic constriction was created by placing a ligature securely around the ascending aorta and a 26-gauge needle and then removing the needle. Sham operated animals underwent the same procedure except for aortic constriction. The animals were extubated after getting a dose of analgesic (buprenorphine, 0.1 mg/kg) subcuta-

neously and allowed to recover. Doppler echocardiography was performed 21 days after primary surgery under general anaesthesia with isoflurane as described above. This time point was selected since previous studies in our laboratory have shown marked hypertrophy in WT mice at this stage. AB mice in both groups with a flow velocity across the aortic banding site greater than 3.5 m/s were included in the study. The same mice anesthetized with isoflurane were euthanized by dislocation of the neck, and the hearts and lungs were removed and blotted dry. The right ventricle and atria were removed. The LV, right ventricular free wall and lungs were weighed and normalized to tibial length.

Doppler Echocardiography

Mice were examined while sedated in the supine position with the chest closed, as previously described [54]. Echocardiography was performed using a i13L 13 MHz linear array transducer (GE Healthcare Technologies, Oslo, Norway) and data were analyzed with EchoPac PC software (GE Healthcare Technologies, Oslo, Norway) as described [55]. The data were recorded and analyzed by a cardiologist (IS), blinded for the genotype.

Isolation of adult myocardial murine cardiomyocytes, fibroblasts and endothelial cells

Mouse cardiomyocytes were isolated as previously described [56]. Endothelial cells were enriched from the non-cardiomyocyte fraction by labeling the cells with a rat anti-mouse CD31 antibody (eBioscience, San Diego, CA) and subsequent extraction using an anti-rat secondary antibody coupled to magnetic beads (Miltenyi Biotec, Auburn, CA) and further column purifications according to the protocols provided by the manufacturer (http://www.miltenyibiotec.com). The cell fraction remaining after extraction of cardiomyocytes and endothelial cells contains predominantly fibroblasts.

RNA isolation

Total RNA was isolated from the LV in WT and CXCR5$^{-/-}$ mice (SV total RNA isolation system, Promega, Inc., Madison, WI), mouse and neonatal rat cardiomyocytes and fibroblasts, and mouse endothelial cells (RNeasy mini kit, Qiagen, Valencia, CA) as previously described [5].

Quantitative real-time PCR (qRT-PCR)

Reverse transcription reactions were performed with iScript Select cDNA Synthesis Kit (Bio-Rad Laboratories, Inc., Hercules, CA). Pre-designed TaqMan assays (Applied Biosystems, Foster City, CA) were used to determine gene expression of CXCL13(Mm00444534_m1), CXCR5 (Mm00432086_m1), ANP (Mm01255748_g1), BNP (Mm00435304_g1), β-MHC (Mm01319006_g1), biglycan (Rn00567229_m1), fibromodlin (Rn00589918_m1), lumican (Rn00579127_m1) and decorin (Rn01503161_m1). The results were detected on an ABI PRISM 7900 Sequence Detection System (Applied Biosystems) as described previously [5]. In the human studies, quantification of gene expression was performed using the ABI Prism 7500 (Applied Biosystems), Power SYBR Green Master Mix (Applied Biosystems), and sequence-specific PCR primers were designed using the Primer Express software, version 3.0 (Applied Biosystems). List of the real-time PCR assays used in the human study is shown in Table S2.

Perfusion fixation and histology

After the hearts were excised and rinsed in cold NaCl solution, the aorta was cannulated, and the hearts were mounted on a Langendorff setup, and retrogradely perfused with warm (37°C) oxygenated Thyrodes solution (5 mM Hepes, pH 7.4, 140 mM NaCl, 5.4 mM KCl, 0.4 MgH_2PO_4, 0.5 $MgCL_2$) with 1.8 mM Ca^{2+}. Hearts were stopped in diastole by aortic perfusion of Thyrodes solution with high KCl (10.8 mM) for 3 min and fixated for 10 min by perfusion of 4% phosphate-buffered formalin. After the cannulas were removed, fixation by immersion continued for 2 h. Each heart was transected at the midventricular level, and both halves were routinely processed and embedded in paraffin. Paired 3.5 μm sections were prepared, mounted on glass slides, and stained with hematoxylin and eosin and Masson tricrome stain.

Hydroxyproline analysis

Quantitative analysis of tissue levels of hydroxyproline was performed by HPLC using the AccQ-Fluor reagent kit (Waters Corporation, Milford, MA) essentially as previously described [57]. Briefly, cardiac tissue samples (5 mg dry weight) were hydrolyzed in 6 M HCl for 16 h at 110°C and subsequently dried under vacuum and redissolved in the AccQ-Fluor borate buffer. Derivatization was initiated by addition of the AccQ-Fluor reagent at 55°C and terminated after 10 min. The samples were finally subjected to HPLC-chromatography using a 20×3.9 mm Sentry Guard column (Nova-Pak C_{18} bonded silica) connected to a 150×3.9 mm AccQ-Tag reversed-phase column (both from Waters) according to the manufacturer's instructions. Derivatized hydroxyproline was detected by fluorescence signal following excitation at 250 nm and recording of emission at 395 nm. Elution of hydroxyproline from myocardial tissue samples was verified and quantified by co-elution with known amounts of derivatized hydroxyproline standards (Fluka, Buchs SG, Switzerland). The relation of myocardial hydroxyproline contents to myocardial collagen has previously been reported [58].

Measurements of total MMP activity and gelatinolytic activity

Total MMP activity in the LV was measured by a fluorogenic peptide substrate (R&D Systems) used to assess broad-range MMP activity (MMP-1, -2, -7, -8, -9, -12 and -13 can cleave the peptide). Gelatinolytic activity was assessed by gelatine zymography. Briefly, the MMP substrate was diluted in TCN buffer (50 mM Tris HCl, 150 mM NaCl, 10 mM $CaCl_2$; pH 7.5) and added to the supernatants before incubation at 37°C. After 120 min the total MMP activity was determined on a fluorimeter (FLX 800 Microplate Fluorescence Reader, Bio-Tek Instruments, Winooski, VT).

Gene expression profiling and microarray data analysis

Total RNA was isolated from the LV in Sham (n = 3) and AB (n = 4) WT and CXCR5$^{-/-}$ mice as described previously [5]. Preparation of cRNA and the subsequent steps leading to hybridization of Affymetrix GeneChip® mouse ST 1.0 arrays (Affymetrix, Santa Clara, CA), washing, and scanning were performed according to standard protocols (Affymetrix). Microarray preprocessing was done using robust multi-array average [59]. Differentially expressed genes were found using significance analysis of microarrays [60]. The seeded Bayesian network method [32] was used to explore interactions between differentially expressed genes. This method finds interactions in the expression data using literature co-citations, databases of protein-protein interactions, as well as co-regulations in the expression data. We constructed two networks; one for the wild type situation, using the 60 most differentially expressed genes between AB WT and SHAM WT, and similarly one for the KO situation, using the

60 most differentially expressed between $CXCR5^{-/-}$ AB and Sham AB. The set of 60 genes were based on a ranking according to fold change (AB *vs.* Sham) using a subset of the genes for which false discovery rate was less than 0.05. All data is MIAME compliant and the following link has been created to allow review of the data in Gene Expression Omnibus (record GSE22295): http://www.ncbi.nlm.nih.gov/geo/query/acc.cgi?token=xdivnmkmeyeiifg&acc=GSE22295

Western blotting

Western blotting was performed as previously described [61] with minor modifications. Snap frozen left ventricles from WT and $CXCR5^{-/-}$ mice were homogenized in cell lysis buffer and equal amounts of protein being separated from each sample by SDS-PAGE (10%) before transferred to polyvinylidene fluoride (PVDF) membranes. Non-specific bindings to the membrane was blocked with 5% BSA for 1 h at room temperature, followed by incubation with anti-fibromodulin (SC-33772; Santa Cruz Biotechnology, Inc., Santa Cruz, CA), anti-decorin (AF1060; R&D Systems, Minneapolis, MN), anti-biglycan (AF2667; R&D) or anti-lumican (AF2745; R&D) overnight at 4°C. The membranes were washed in TBS-T and followed by species-specific horseradish peroxidase-coupled secondary antibodies in 5% BSA added for 1 h. After washing, the immune complexes were visualized by ECL (GE Healthcare, Buckinghamshire, UK) and the membranes were exposed to x-ray film (HyperfilmTM ECL, GE healthcare) and developed. Immunoblots were stripped and re-probed with anti-GAPDH (C20357; R&D) for normalization. Filters with LV lysate were also probed with antibody against P-ERK1/2 (Phospho-p44/42 MAP kinase (Thr 202/Tyr 204), Cell Signaling Technology, Danvers, MA) or p44/42 MAP kinase (Cell Signaling Technology) followed by species-specific horseradish peroxidase-coupled secondary antibodies (Cell Signaling). The immune complexes were visualized with the use of Supersignal West Pico (Pierce, Rockford, IL) and exposed films were detected by using Kodak 440 CF imaging station (Boston, MA). The software Total Laboratory v.1*10 (Phoretix, Newcastle, UK) was used for quantification.

Transmission electron microscopy

For transmission electron microscopy, hearts (n = 2) from each group were perfused with 2.0% glutaraldehyde buffered in 0.2 M cacodylate at pH 7.4 for 15 min. Small blocks (about 3 mm^3 in size) of the LV and septum were taken. The tissues were fixated in cacodylate buffer for 2 h and washed in the same buffer 3 times. The blocks of tissue were then transferred to a 1% OsO_4 solution for 10 min on ice. After washing in cacodylate, dehydration was carried out rapidly in graded ethanol series, followed by embedding in Epon. Sections were cut at a thickness of 60–100 nm and collected on 200 mesh grids, and stained with uranyl acetat for 7 minutes and lead for 3 minutes. The sections were examined and photographed in a Tecnai G2 spirit BioTWIN 120 kV, LaB6, Transmission Electron Microscope with 4k Eagle camera from FEI Company. We obtained micrographs of the LV septum and the free wall at different magnifications.

TUNEL Staining

TUNEL staining was performed on paraffin-embedded sections using the *In Situ* Cell Death Detection kit (Roche Diagnostics) as described [62]. Briefly, paraffin-embedded (6 µm) sections of mouse hearts were deparaffinized in xylene, rehydrated, and treated with 0.5% Triton X-100 in 0.1% Na-citrate for 30 min. After several washes with PBS, the sections were permeabilized with proteinase K (20 µg/ml in TE, pH 8.0) for 30 min at 37°C. Subsequently, the sections were rinsed with PBS, and the area around the sample was dried. TUNEL reaction mixture (50 µl) containing terminal deoxynucleotidyl transferase was applied and tissue sections were incubated in a dark, humidified chamber for 1 h at 37°C. After several washes with PBS the tissue sections were analyzed with a fluorescence microscope (515–565 nm). A quantitative analysis (number of apoptotic cells/total number of cells counted) was performed by counting cells in a randomly selected area of each tissue sample.

Immunohistochemistry

Paired 3.5 µm sections were immunostained using affinity-purified rabbit polyclonal CD3 antibody (Abcam, Cambridge, U.K.), dilution 1:400, and anti-mouse/human CD45R (eBioscience, San Diego, CA), dilution 1:4500. The immune reaction was visualized using horseradish peroxidase in a Dako Autostainer plus (Dako, Glostrup, Denmark). We obtained 32 digital images of evenly distributed microscopic high power fields (×400) from the left ventricular free wall and ventricular septum of six heart sections in each group. The sections were from no less than three hearts in each group. The 32 images from each heart were studied by two investigators (AW and HMR), blinded for mouse identity, counting the total number of CD3 and CD45R positive lymphocytes.

Isolation and stimulation of neonatal myocardial rat fibroblasts

Primary neonatal fibroblasts were isolated from 1–3 day old Wistar rats (Taconic, Skensved, Denmark). Briefly, fibroblasts were separated by Percoll density gradient and transferred to plating medium and maintained in culture for up to 96 hours. The fibroblasts were stimulated with human recombinant CXCL13, 200 ng/ml (R&D Systems, Minneapolis, MN), with or without the ERK1/2 inhibitor (10 µM final concentration UO126 (MEK inhibitor, Promega, WI)), for 3 and 20 hours before storing cell pellet (mRNA analyses) and cell-free supernatant (MMP activity) at −80°C until further analyses. Un-stimulated (control) cells were also given vehicle. The toxicity in cell cultures was examined routinely for lactate dehydrogenase leakage using a cytotoxicity detection kit (Roche Applied Science, Mannheim, Germany).

P-ERK1/2 (Phospho-p44/42 MAP kinase) and ERK1/2 (p44/42 MAP kinase) detection

Phospho-p44/42 MAP kinase and p44/42 MAP kinase levels in left ventricle lysate were measured by multiplex suspension array technology using the BioPlex (Bio-Rad, Hercules, CA). Phospho-p44/42 MAP kinase and p44/42 MAP kinase multiplexable beads were purchased from R&D Systems. The quantification was accomplished by using the BioPlex Manager Software (Bio-Rad).

Tissue sampling from human myocardium

In nine patients with advanced HF (NYHA class IV; 8 male, 1 female; age 29±5 years), LV tissue was available at the time of implantation and at the time of removal (heart transplantation) of a continuous-flow LV assist device (LVAD; EntrAssist, Ventracor Ltd, Chatswood, Australia). Average time on LVAD was 8±1.7 months. Control (non-failing) human LV tissue was obtained from subjects whose hearts were rejected as cardiac donors for surgical reasons (n = 5). The cause of death of donors was cerebrovascular accident, and none had a history of heart disease. Myocardium from these subjects was kept on ice for 1 to 4 hours before tissue sampling was conducted. In both failing and non-failing myocardium, LV tissue samples were snap-frozen in liquid nitrogen, and stored at −80°C until use. None of patients (failing

and non-failing myocardium) had significant concomitant disease such as infection, malignancy, or autoimmune disorder.

Supporting Information

Figure S1 Altered expression of markers of cardiac wall stress and remodeling. Relative gene expression of (**A**) atrial natriuretic peptide (ANP), (**B**) brain natriuretic peptide (BNP) and (**C**) β-myosin heavy chain (MHC) in wild type (WT) Sham (n = 6), $CXCR5^{-/-}$ Sham (n = 6), WT aorta banded (AB) (n = 6), and $CXCR5^{-/-}$ AB (n = 6) groups. The results are mean ± SEM. *p<0.05 and ***p<0.001 *vs.* Sham groups; †p<0.05 and †††p <0.001 *vs.* WT AB group.
(TIF)

Figure S2 Fluorescent micrographs of sections of left ventricular myocardium from wild type (WT) and $CXCR5^{-/-}$ mice. The arrows indicate TUNEL-positive myocyte nucleus.
(TIF)

Figure S3 CD45 and CD3 positive lymphocytes in the left ventricular myocardium from wild type (WT) and $CXCR5^{-/-}$ mice. Total number of CD45R (**A**) and CD3 (**B**) postive lymphocytes was not significantly different between $CXCR5^{-/-}$ and WT mice after sham operation or AB. (n = 6 heart sections in all groups). Cells counted from 32 digital, evenly distributed images (x400) from each heart.The results are mean ± SEM.
(TIF)

Table S1 Weights and echocardiographic measurements. Values are means ± SE. BW, body weight; TL, tibia length; LVW, left ventricular weight; LW, lung weight; IVSd and IVSs, interventricular septum thickness in diastole and in systole, respectively; LVD_d and LVD_s, left ventricular diameter in diastole and in systole, respectively; FS, fractional shortening in LVD; LVPWd and LVPWs, posterior wall thickness in diastole and in systole, respectively; LAD, left atrial diameter; HR, heart rate; AVmax, peak aortic stenosis flow velocity; TVs, peak tissue velocity in systole; TVd, peak tissue velocity in diastole. LVW/TL and LW/TL are mg/mm. * p<0.05, ** p<0.01, *** p<0.001 vs. Non-operated and Sham groups. †p<0.05, ††, p <0.01, †††p<0.001 vs. WT AB group. ‡p<0.05 vs $CXCR5^{-/-}$ Non-operated group. The results are mean ± SEM.
(DOC)

Table S2 Characteristics of the real-time PCR assays used in the human study. The table shows the sequence of primers used in the real-time PCR assays. (+), forward primers; (–), reverse primers; Acc.nr, GenBank accession number; GAPDH, glyceraldehyde 3-phosphate dehydrogenase.
(DOC)

Acknowledgments

We thank Bjørg Austbø, Dina Behmen, Sigurd Boye, Ulla Enger, Geir Florholmen, Eli Wallem Gulliksen, Tove Noren, Ole Kristoffer Olstad, Anett Hellebø Ottesen, Ellen Lund Sagen and Kalpana Sinnadurai for excellent assistance.

Author Contributions

Conceived and designed the experiments: AW GC BH AY PA. Performed the experiments: AW BH AY CH AVF HR MSA DH-K WEL. Analyzed the data: AW BH GC PA IS SN HA MSA BR HR LEV. Contributed reagents/materials/analysis tools: ML. Wrote the paper: AW GC PA. Collected humane data and commented on the manuscript: CPD LG.

References

1. Aukrust P, Ueland T, Lien E, Bendtzen K, Müller F, et al. (1999) Cytokine network in congestive heart failure secondary to ischemic or idiopathic dilated cardiomyopathy. Am J Cardiol 83: 376–382.
2. Torre-Amione G, Kapadia S, Lee J, Durand JB, Bies RD, et al. (1996) Tumor necrosis factor-alpha and tumor necrosis factor receptors in the failing human heart. Circulation 93: 704–711.
3. Damås JK, Gullestad L, Aass H, Simonsen S, Fjeld JG, et al. (2001) Enhanced gene expression of chemokines and their corresponding receptors in mononuclear blood cells in chronic heart failure—modulatory effect of intravenous immunoglobulin. J Am Coll Cardiol 38: 187–193.
4. Woldbæk PR, Sande JB, Strømme TA, Lunde PK, Djurovic S, et al. (2005) Daily administration of interleukin-18 causes myocardial dysfunction in healthy mice. Am J Physiol Heart Circ Physiol 289: H708–H714.
5. Husberg C, Nygard S, Finsen AV, Damås JK, Frigessi A, et al. (2008) Cytokine expression profiling of the myocardium reveals a role for CX3CL1 (fractalkine) in heart failure. J Mol Cell Cardiol 45: 261–269.
6. Mann DL (2001) Recent insights into the role of tumor necrosis factor in the failing heart. Heart Fail Rev 6: 71–80.
7. Matsumori A, Sasayama S (2001) The role of inflammatory mediators in the failing heart: immunomodulation of cytokines in experimental models of heart failure. Heart Fail Rev 6: 129–136.
8. Dibbs Z, Kurrelmeyer K, Kalra D, Seta Y, Wang F, et al. (1999) Cytokines in heart failure: pathogenetic mechanisms and potential treatment. Proc Assoc Am Physicians 111: 423–428.
9. Förster R, Emrich T, Kremmer E, Lipp M (1994) Expression of the G-protein—coupled receptor BLR1 defines mature, recirculating B cells and a subset of T-helper memory cells. Blood 84: 830–840.
10. Förster R, Davalos-Misslitz AC, Rot A (2008) CCR7 and its ligands: balancing immunity and tolerance. Nat Rev Immunol 8: 362–371.
11. Müller G, Höpken UE, Lipp M (2003) The impact of CCR7 and CXCR5 on lymphoid organ development and systemic immunity. Immunol Rev 195: 117–135.
12. Ohl L, Henning G, Krautwald S, Lipp M, Hardtke S, et al. (2003) Cooperating mechanisms of CXCR5 and CCR7 in development and organization of secondary lymphoid organs. J Exp Med 197: 1199–1204.
13. Ebert LM, Schaerli P, Moser B (2005) Chemokine-mediated control of T cell traffic in lymphoid and peripheral tissues. Mol Immunol 42: 799–809.
14. Förster R, Mattis AE, Kremmer E, Wolf E, Brem G, et al. (1996) A putative chemokine receptor, BLR1, directs B cell migration to defined lymphoid organs and specific anatomic compartments of the spleen. Cell 87: 1037–1047.
15. Cyster JG, Ansel KM, Reif K, Ekland EH, Hyman PL, et al. (2000) Follicular stromal cells and lymphocyte homing to follicles. Immunol Rev 176: 181–193.
16. Gunn MD, Ngo VN, Ansel KM, Ekland EH, Cyster JG, et al. (1998) A B-cell-homing chemokine made in lymphoid follicles activates Burkitt's lymphoma receptor-1. Nature 391: 799–803.
17. Weyand CM, Goronzy JJ (2003) Ectopic germinal center formation in rheumatoid synovitis. Ann N Y Acad Sci 987: 140–149.
18. Ansel KM, Heyzer-Williams LJ, Ngo VN, Heyzer-Williams MG, Cyster JG (1999) In vivo-activated CD4 T cells upregulate CXC chemokine receptor 5 and reprogram their response to lymphoid chemokines. J Exp Med 190: 1123–1134.
19. Haynes NM, Allen CD, Lesley R, Ansel KM, Killeen N, et al. (2007) Role of CXCR5 and CCR7 in follicular Th cell positioning and appearance of a programmed cell death gene-1high germinal center-associated subpopulation. J Immunol 179: 5099–5108.
20. Schmutz C, Hulme A, Burman A, Salmon M, Ashton B, et al. (2005) Chemokine receptors in the rheumatoid synovium: upregulation of CXCR5. Arthritis Res Ther 7: R217–R229.
21. Qiuping Z, Jie X, Youxin J, Qun W, Wei J, et al. (2005) Selectively frequent expression of CXCR5 enhances resistance to apoptosis in CD8(+)CD34(+) T cells from patients with T-cell-lineage acute lymphocytic leukemia. Oncogene 24: 573–584.
22. Shi K, Hayashida K, Kaneko M, Hashimoto J, Tomita T, et al. (2001) Lymphoid chemokine B cell-attracting chemokine-1 (CXCL13) is expressed in germinal center of ectopic lymphoid follicles within the synovium of chronic arthritis patients. J Immunol 166: 650–655.
23. Amft N, Curnow SJ, Scheel-Toellner D, Devadas A, Oates J, et al. (2001) Ectopic expression of the B cell-attracting chemokine BCA-1 (CXCL13) on endothelial cells and within lymphoid follicles contributes to the establishment of germinal center-like structures in Sjogren's syndrome. Arthritis Rheum 44: 2633–2641.
24. Salomonsson S, Larsson P, Tengner P, Mellquist E, Hjelmström P, et al. (2002) Expression of the B cell-attracting chemokine CXCL13 in the target organ and autoantibody production in ectopic lymphoid tissue in the chronic inflammatory disease Sjogren's syndrome. Scand J Immunol 55: 336–342.
25. Xanthou G, Polihronis M, Tzioufas AG, Paikos S, Sideras P, et al. (2001) "Lymphoid" chemokine messenger RNA expression by epithelial cells in the chronic inflammatory lesion of the salivary glands of Sjogren's syndrome patients: possible participation in lymphoid structure formation. Arthritis Rheum 44: 408–418.

26. Carlsen HS, Baekkevold ES, Johansen FE, Haraldsen G, Brandtzaeg P (2002) B cell attracting chemokine 1 (CXCL13) and its receptor CXCR5 are expressed in normal and aberrant gut associated lymphoid tissue. Gut 51: 364–371.
27. Festa ED, Hankiewicz K, Kim S, Skurnick J, Wolansky LJ, et al. (2009) Serum levels of CXCL13 are elevated in active multiple sclerosis. Mult Scler.
28. Dobner T, Wolf I, Emrich T, Lipp M (1992) Differentiation-specific expression of a novel G protein-coupled receptor from Burkitt's lymphoma. Eur J Immunol 22: 2795–2799.
29. Meijer J, Zeelenberg IS, Sipos B, Roos E (2006) The CXCR5 chemokine receptor is expressed by carcinoma cells and promotes growth of colon carcinoma in the liver. Cancer Res 66: 9576–9582.
30. Singh S, Singh R, Singh UP, Rai SN, Novakovic KR, et al. (2009) Clinical and biological significance of CXCR5 expressed by prostate cancer specimens and cell lines. Int J Cancer 125: 2288–2295.
31. Tyagi SC (1998) Extracellular matrix dynamics in heart failure: a prospect for gene therapy. J Cell Biochem 68: 403–410.
32. Djebbari A, Quackenbush J (2008) Seeded Bayesian Networks: constructing genetic networks from microarray data. BMC Syst Biol 2: 57.
33. Hocking AM, Shinomura T, McQuillan DJ (1998) Leucine-rich repeat glycoproteins of the extracellular matrix. Matrix Biol 17: 1–19.
34. Svensson L, Aszodi A, Reinholt FP, Fassler R, Heinegard D, et al. (1999) Fibromodulin-null mice have abnormal collagen fibrils, tissue organization, and altered lumican deposition in tendon. J Biol Chem 274: 9636–9647.
35. Danielson KG, Baribault H, Holmes DF, Graham H, Kadler KE, et al. (1997) Targeted disruption of decorin leads to abnormal collagen fibril morphology and skin fragility. J Cell Biol 136: 729–743.
36. Hu C, Xiong J, Zhang L, Huang B, Zhang Q, et al. (2004) PEG10 activation by co-stimulation of CXCR5 and CCR7 essentially contributes to resistance to apoptosis in CD19+CD34+ B cells from patients with B cell lineage acute and chronic lymphocytic leukemia. Cell Mol Immunol 1: 280–294.
37. Chunsong H, Yuling H, Li W, Jie X, Gang Z, et al. (2006) CXC chemokine ligand 13 and CC chemokine ligand 19 cooperatively render resistance to apoptosis in B cell lineage acute and chronic lymphocytic leukemia CD23+CD5+ B cells. J Immunol 177: 6713–6722.
38. Legler DF, Loetscher M, Roos RS, Clark-Lewis I, Baggiolini M, et al. (1998) B cell-attracting chemokine 1, a human CXC chemokine expressed in lymphoid tissues, selectively attracts B lymphocytes via BLR1/CXCR5. J Exp Med 187: 655–660.
39. Moser B, Schaerli P, Loetscher P (2002) CXCR5(+) T cells: follicular homing takes center stage in T-helper-cell responses. Trends Immunol 23: 250–254.
40. Yamazaki T, Komuro I, Yazaki Y (1998) Signalling pathways for cardiac hypertrophy. Cell Signal 10: 693–698.
41. Müller G, Lipp M (2001) Signal transduction by the chemokine receptor CXCR5: structural requirements for G protein activation analyzed by chimeric CXCR1/CXCR5 molecules. Biol Chem 382: 1387–1397.
42. Damås JK, Eiken HG, Oie E, Bjerkeli V, Yndestad A, et al. (2000) Myocardial expression of CC- and CXC-chemokines and their receptors in human end-stage heart failure. Cardiovasc Res 47: 778–787.
43. Dahl CP, Husberg C, Gullestad L, Waehre A, Damås JK, et al. (2009) Increased production of CXCL16 in experimental and clinical heart failure: a possible role in extracellular matrix remodeling. Circ Heart Fail 2: 624–632.
44. Monfort J, Tardif G, Reboul P, Mineau F, Roughley P, et al. (2006) Degradation of small leucine-rich repeat proteoglycans by matrix metalloprotease-13: identification of a new biglycan cleavage site. Arthritis Res Ther 8: R26.
45. Morimoto H, Takahashi M, Izawa A, Ise H, Hongo M, et al. (2006) Cardiac overexpression of monocyte chemoattractant protein-1 in transgenic mice prevents cardiac dysfunction and remodeling after myocardial infarction. Circ Res 99: 891–899.
46. Tachibana K, Hirota S, Iizasa H, Yoshida H, Kawabata K, et al. (1998) The chemokine receptor CXCR4 is essential for vascularization of the gastrointestinal tract. Nature 393: 591–594.
47. Doi M, Kusachi S, Murakami T, Ninomiya Y, Murakami M, et al. (2000) Time-dependent changes of decorin in the infarct zone after experimentally induced myocardial infarction in rats: comparison with biglycan. Pathol Res Pract 196: 23–33.
48. Yamamoto K, Kusachi S, Ninomiya Y, Murakami M, Doi M, et al. (1998) Increase in the expression of biglycan mRNA expression Co-localized closely with that of type I collagen mRNA in the infarct zone after experimentally-induced myocardial infarction in rats. J Mol Cell Cardiol 30: 1749–1756.
49. Weis SM, Zimmerman SD, Shah M, Covell JW, Omens JH, et al. (2005) A role for decorin in the remodeling of myocardial infarction. Matrix Biol 24: 313–324.
50. Westermann D, Mersmann J, Melchior A, Freudenberger T, Petrik C, et al. (2008) Biglycan is required for adaptive remodeling after myocardial infarction. Circulation 117: 1269–1276.
51. Bueno OF, De Windt LJ, Tymitz KM, Witt SA, Kimball TR, et al. (2000) The MEK1-ERK1/2 signaling pathway promotes compensated cardiac hypertrophy in transgenic mice. EMBO J 19: 6341–6350.
52. Sanna B, Bueno OF, Dai YS, Wilkins BJ, Molkentin JD (2005) Direct and indirect interactions between calcineurin-NFAT and MEK1-extracellular signal-regulated kinase 1/2 signaling pathways regulate cardiac gene expression and cellular growth. Mol Cell Biol 25: 865–878.
53. Ding B, Price RL, Borg TK, Weinberg EO, Halloran PF, et al. (1999) Pressure overload induces severe hypertrophy in mice treated with cyclosporine, an inhibitor of calcineurin. Circ Res 84: 729–734.
54. Sjaastad I, Sejersted OM, Ilebekk A, Bjørnerheim R (2000) Echocardiographic criteria for detection of postinfarction congestive heart failure in rats. J Appl Physiol 89: 1445–1454.
55. Finsen AV, Christensen G, Sjaastad I (2005) Echocardiographic parameters discriminating myocardial infarction with pulmonary congestion from myocardial infarction without congestion in the mouse. J Appl Physiol 98: 680–689.
56. Vinge LE, von Lueder TG, Aasum E, Qvigstad E, Gravning JA, et al. (2008) Cardiac-restricted expression of the carboxyl-terminal fragment of GRK3 uncovers distinct functions of GRK3 in regulation of cardiac contractility and growth: GRK3 controls cardiac alpha1-adrenergic receptor responsiveness. J Biol Chem 283: 10601–10610.
57. Liu H, Sanuda-Pena MC, Harvey-White JD, Kalra S, Cohen SA (1998) Determination of submicromolar concentrations of neurotransmitter amino acids by fluorescence detection using a modification of the 6-aminoquinolyl-N-hydroxysuccinimidyl carbamate method for amino acid analysis. J Chromatogr A 828: 383–395.
58. Laurent GJ, Cockerill P, McAnulty RJ, Hastings JR (1981) A simplified method for quantitation of the relative amounts of type I and type III collagen in small tissue samples. Anal Biochem 113: 301–312.
59. Irizarry RA, Hobbs B, Collin F, Beazer-Barclay YD, Antonellis KJ, et al. (2003) Exploration, normalization, and summaries of high density oligonucleotide array probe level data. Biostatistics 4: 249–264.
60. Tusher VG, Tibshirani R, Chu G (2001) Significance analysis of microarrays applied to the ionizing radiation response. Proc Natl Acad Sci U S A 98: 5116–5121.
61. Finsen AV, Woldbæk PR, Li J, Wu J, Lyberg T, et al. (2004) Increased syndecan expression following myocardial infarction indicates a role in cardiac remodeling. Physiol Genomics 16: 301–308.
62. Calvert JW, Zhou C, Nanda A, Zhang JH (2003) Effect of hyperbaric oxygen on apoptosis in neonatal hypoxia-ischemia rat model. J Appl Physiol 95: 2072–2080.

Waehre *et al.* CXCL13/CXCR5 in heart failure

SUPPLEMENTARY INFORMATION

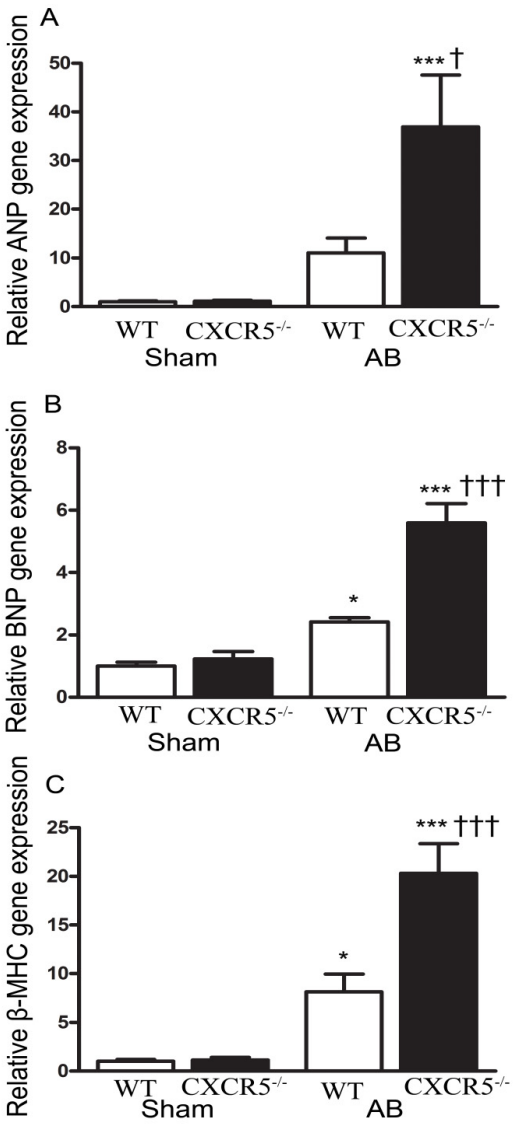

Figure S1. Altered expression of markers of cardiac wall stress and remodeling. Relative gene expression of (**A**) atrial natriuretic peptide (ANP), (**B**) brain natriuretic peptide (BNP) and (**C**) β-myosin heavy chain (MHC) in wild type (WT) Sham (n=6), CXCR5$^{-/-}$ Sham (n=6), WT aorta banded (AB) (n=6), and CXCR5$^{-/-}$ AB (n=6) groups. The results are mean ± SEM. *p<0.05 and ***p<0.001 *vs*. Sham groups; †p<0.05 and †††p <0.001 *vs*. WT AB group.

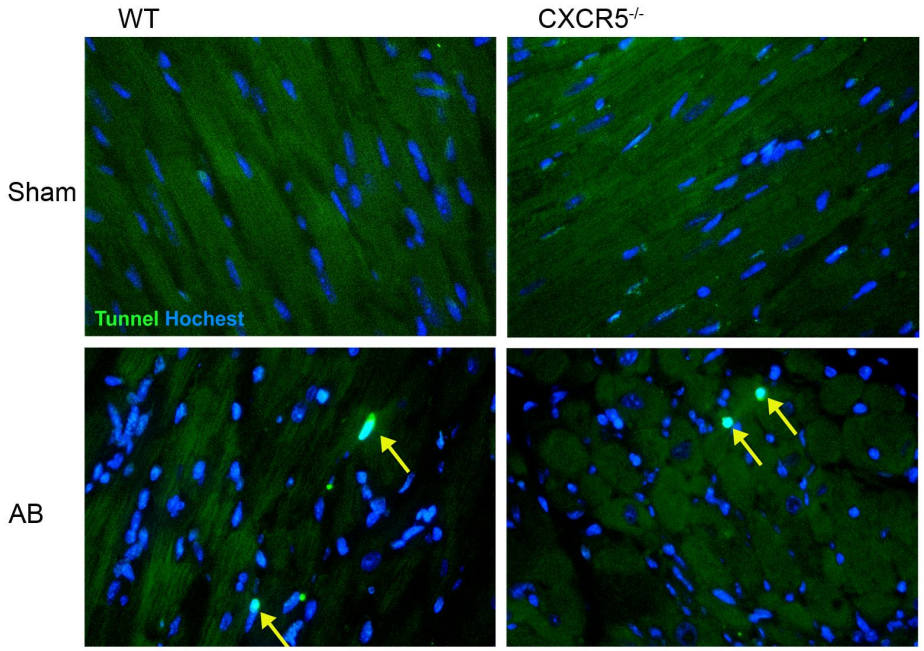

Figure S2. Fluorescent micrographs of sections of left ventricular myocardium from wild type (WT) and CXCR5$^{-/-}$ mice. The arrows indicate TUNEL-positive myocyte nucleus.

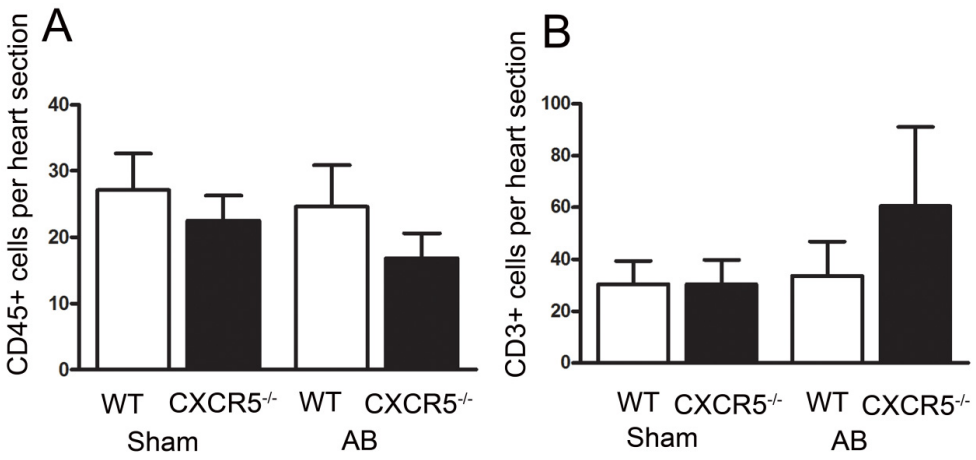

Figure S3. Total number of CD45R (**A**) and CD3 (**B**) postive lymphocytes was not significantly different between CXCR5$^{-/-}$ and WT mice after sham operation or AB. (n=6 heart sections in all groups). Cells counted from 32 digital, evenly distributed images (x400) from each heart.The results are mean ± SEM.

Table S1. Weights and echocardiographic measurements

	WT	CXCR5$^{-/-}$	WT Sham	CXCR5$^{-/-}$ Sham	WT AB	CXCR5$^{-/-}$ AB
n	6	6	7	7	6	8
Weights						
BW (g)	26.2±0.8	25.3±0.7	27.9±0.9	25.8±0.9	27.8±1.0	26.4±0.6
TL (mm)	18.2±0.1	17.3±0.3	18.0±0.1	17.6±0.1	18.3±0.1	17.3±0.4
LVW/TL	5.4±0.2	5.2±0.3	5.5±0.2	5.3±0.3	8.6±0.5***	8.6±0.3**
LW/TL	8.9±0.2	9.0±0.5	8.7±0.2	9.1±0.5	17.6±2.5**	16.0±2.7*
Echocardiography						
M-Mode						
IVSd (mm)	0.56±0.09	0.56±0.06	0.68±0.07	0.62±0.03	0.98±0.18**	0.67±0.12†
IVSs (mm)	0.87±0.08	0.83±0.15	1.02±0.13	0.96±0.17	1.38±0.27***	0.79±0.16†††
LVIDd (mm)	4.50±0.37	4.28±0.17	4.43±0.30	4.59±0.32	4.31±0.29	5.40±0.59*†
LVIDs (mm)	3.63±0.42	3.42±0.22	3.54±0.56	3.68±0.25	3.43±0.47	5.03±0.80**†††
FS (%)	19.13±4.55	20.25±4.07	20.86±2.34	19.67±1.03	20.50±5.75	7.50±5.21*†
LVPWd (mm)	0.63±0.09	0.61±0.06	0.67±0.15	0.60±0.11	1.10±0.22***	0.68±0.14†††
LVPWs (mm)	0.84±0.09	0.76±0.10	0.98±0.19	0.79±0.07	1.36±0.16***	0.87±0.22†††
LAD (mm)	1.59±0.2	1.78±0.14	1.73±0.14	1.71±0.09	2.58±0.55***	3.17±0.41***
Doppler						
HR (BMP)	430.3±78.03	471.8±36.3	417.6±29.2	433.3±58.4	453.8±92.7	463.5±68.9
AVmax (m/s)					4.12±0.19	4.33±0.54
TVs (cm/s)	1.33±0.37	1.54±0.30	1.18±0.35	1.11±0.16‡	0.77±0.28***	0.66±0.31***
TVd (cm/s)	1.50±0.27	1.63±0.19	1.18±0.60	0.99±0.18	0.91±0.47	0.73±0.38**

Table S1. Values are means ± SE. BW, body weight; TL, tibia length; LVW, left ventricular weight; LW, lung weight; IVSd and IVSs, interventricular septum thickness in diastole and in systole, respectively; LVD_d and LVD_s, left ventricular diameter in diastole and in systole, respectively; FS, fractional shortening in LVD; LVPWd and LVPWs, posterior wall thickness in diastole and in systole, respectively; LAD, left atrial diameter; HR, heart rate; AVmax, peak aortic stenosis flow velocity; TVs, peak tissue velocity in systole; TVd, peak tissue velocity in diastole. LVW/TL and LW/TL are mg/mm. * $p<0.05$, ** $p<0.01$, *** $p<0.001$ vs. Non-operated and Sham groups. †$p<0.05$, ††, $p<0.01$, †††$p<0.001$ vs. WT AB group. ‡$p<0.05$ vs CXCR5$^{-/-}$ Non-operated group. The results are mean ± SEM.

Table S2. Real-time PCR assays in the human study

Target	Sequence (5'→3')	Acc.Nr.
Biglycan	(+)-GAATGAACTCCACCTAGACCACAAC	NM_001711
	(–)-AGGCCCAGCCTGTACAGCTT	
CXCR5	(+)-GCCGGCACAGCCATGA	NM_001716
	(–)-CTGTCCAGTTCCCAGAACAGGT	
Fibromodulin	(+)-CTCTCCCAGGCCCAGTATGA	NM_002023
	(–)-TAAGGGTCATAGGGATCGTAGTAGGT	
GAPDH	(+)-CCAAGGTCATCCATGACAACTT	NM_002046
	(–)-AGGGGCCATCCACAGTCTT	
Lumican	(+)-GGGCAATCATCACCAAACTGT	NM_002345
	(–)-AGGAGGCACCATTGGTACACTT	

Table S2. Characteristics of the real-time PCR assays used in the human study. The table shows the sequence of primers used in the real-time PCR assays. (+), forward primers; (–), reverse primers; Acc.nr, GenBank accession number; GAPDH, glyceraldehyde 3-phosphate dehydrogenase.

III

IV